Peer-reviewed version available at Sustainability 2018, 10, 2303; doi:10.3390/su10072303

Article

Regional Differences in Energy and Environmental Performance: An Empirical Study of 283 Cities in China

Zuoren Sun[1,*], Chao An[1] and Huachen Sun[2,*]

[1] Business School, Shandong University, Weihai, No. 180 West Culture Road, Weihai 264209, China;
[2] Shandong Academy of Macroeconomic Research, No. 9 South Qianfoshan Road, Jinan 250014, China;
* Correspondence: sunzuoren@sdu.edu.cn (Z.S.); shc82623598@126.com (H.S.); Tel: +86-139-6312-2745 (Z.S.); +86-176-8661-8088 (H.S.); Fax: +86-63-1568-8289

Abstract: This paper proposes a new non-radial biennial Luenberger energy and environmental performance index (EEPI) to measure the EEP change in various Chinese cities. The sources of EEP change, in terms of technical efficiency change and technological change, are examined by Luenberger EEPI. The contributions from specific undesirable outputs and energy inputs to the EEP change are identified by means of the non-radial efficiency measure. The proposed approach is applied to evaluate the EEP of the industrial sector in 283 cities in China over 2010-2014. Factors influencing the emission abatement potential are investigated by employing geographically weighted regression (GWR) model. We find that 1) changes in EEP can be attributed to technological progress but that technological progress slows down across the study period; 2) the soot emission performance experiences a downtrend among four specific sub-performances in line with the truth that severe haze happened frequently in China; 3) the best performers begin to move from the coastal to inland cities with the less resource consumption and higher ecological equality; 4) cities with the strongest positive effect in regards to pollution intensity on emission abatement potential are located in the areas around the Bohai Gulf, where air pollution is particularly severe.

Keywords: data envelopment analysis; biennial Luenberger index; geographically weighted regression; EEP

1. Introduction

With the globalization, China accelerates melting into the world economy after entering WTO and becomes world factory in international division with rapid economic growth. However, this growth is mainly driven by development within the energy-intensive industrial sector [1]. According to the BP Statistical Review of World Energy 2017 [2], China is currently the world's largest energy consumer at 23% of the total global consumption and 27% of the demand growth of global energy consumption in 2016. However, China has paid a high price to the environment for such rapid advancement. Uncontrolled fossil fuel combustion has released poisonous substances in various forms and led to all kinds of pollutions [3], e.g., water contamination, acid rain, and haze (smog). Massive loads of waste gases have been emitted into the atmosphere to create a severe decline in air quality.

China has suffered from severe haze over many of its cities comprised of fine particulate matter less than 2.5 micrometers in diameter (PM2.5), especially in winter months, since 2013. In 2016, only 84 Chinese cities had standard air quality – this amounts to merely 24.9% among the 338 monitored cities at or above the prefecture level (Report on the State of China's Environment in 2016 [4]). Pollution severely affects Chinese citizens' daily living conditions and, ultimately, threatens their health. Epidemiological studies have revealed a strong association between exposure to fine

particulate matter and mortality [5, 6]. Many environmental laws and regulations have been enacted to combat this, including China's State Council's *Action Plan for Air Pollution Prevention and Control* [1]targeting air quality in September 2013. One goal of the Action Plan is to reduce the annual average concentration of fine particulate matter by 25% in the Beijing-Tianjin-Hebei region by 2017 against the 2012 level. Measuring energy efficiency and environmental efficiency can provide quantitative information for energy and environmental policy analysis and decision-making. Cities are not only energy-consumptive, but also form the main sources of various pollutants. Cities, to this effect, are the main battlefield for controlling pollutant emissions. It is essential for administrators to understand the energy and environmental performance (EEP) of their cities to formulate scientific, strategic goals for energy conservation and emission reduction.

In recent years, the data envelopment analysis (DEA) linear programming method has become a popular approach to measuring energy and environmental efficiency to reduce energy consumption and control emissions. DEA was proposed by Farrell [7] and developed by Charnes, et al. [8] to automatically generate appropriate production functions to combine multiple inputs and multiple outputs. The principle of DEA is to enable data to "speak for itself" rather than necessitate excessive artificial parametric assumptions for functions [9]. Many previous researchers have studied energy efficiency; Hu and Wang [10], for example, first established the total factor energy efficiency (TFEE) concept by using DEA. Song, et al. [11] used a bootstrap-DEA approach to find that China's energy efficiency has maintained a slow upward trend from 1992 to 2010. Özkara and Atak [12], and later Feng and Wang [13], measured total-factor energy efficiency and energy savings potential in Turkey's manufacturing industry and China's provincial industrial sectors, respectively. Zhou, et al. [14] proposed an output-specific energy efficiency estimating method. These researchers concentrated on static analysis without dynamic comparison. Honma and Hu [15] investigated the dynamic changes in energy efficiency by introducing a Malmquist productivity index (MPI). Other researchers, such as Wang and Zhou [16], Chang and Hu [17], and Zhang, et al. [18] have made dynamic analyses of energy efficiency as well.

Beside above energy efficiency evaluation models, researchers center around securing as many desirable outputs as possible while minimizing the undesirable outputs which are inevitably produced by industrial production. Färe, et al. [19] first proposed the concept of environmental DEA technology to incorporate undesirable outputs into efficiency evaluation frameworks. Kuosmanen and Kortelainen [9] applied DEA to aggregate multiple undesirable outputs and emphasized the trade-off between economic production and environmental protection in regards to the impact of undesirable outputs on the economy. Kortelainen [20] extended the static framework to a dynamic environmental performance analysis by using MPI; they decomposed the changes in environmental performance into two components: relative environmental efficiency change and relative environmental technological change.

Many previous researchers have used the radial DEA approach to measure environmental performance, where in different undesirable outputs are adjusted by the same proportion. However, radial efficiency measures overestimate technical efficiency due to the existence of nonzero slacks. A series of non-radial DEA models have been developed to resolve this limitation. For example, Zhou, et al. [21] employed a non-radial DEA approach to measure the environmental performance of OECD countries. Zhang and Choi [22] explored total-factor carbon emission performance in China's fossil fuel power plants using a metafrontier non-radial MPI. Rashidi and Saen [23] calculated the pure eco-efficiency of OECD countries by a non-radial DEA model based on green indicators. Sueyoshi and Goto [24] applied a non-radial DEA environmental assessment to evaluate the performance of coal-fired power plants in the northeast United States. Xie, et al. [25] computed environmental efficiency based on a directional distance function with the radial and non-radial slacks of outputs.

There are two major approaches to estimating productivity or efficiency changes: the Malmquist productivity index and Luenberger productivity index. Some researchers assert that the Malmquist productivity index overestimates productivity changes compared to the Luenberger [26, 27]. Further,

[1] One could refer to http://www.gov.cn/zwgk/2013-09/12/content_2486773.htm for more details.

the Luenberger productivity index is a difference-based index, so it is well applicable to measuring differences in EEP. Recent researchers have adapted the Luenberger productivity index to study dynamic changes in productivity or efficiency. For instance, Mahlberg and Sahoo [28] applied non-radial decompositions of the Luenberger productivity index to analyze the eco-productivity performance behavior in 22 OECD countries. Based on a Luenberger environmental index, Azad and Ancev [29] measured the relative environmental efficiency of agricultural water use to reveal substantial variations across different regions. Wang [30] applied the Luenberger index to explore changes in energy and environmental productivity at the provincial level. Our research team developed a non-radial Luenberger productivity index to resolve the limitation of radial measurement [31, 32]. Non-radial efficiency measures can help us identify specific effects and contributions of energy factor and specific undesirable outputs, while radial efficiency measures do not reflect the impact of emission structures on efficiency changes.

The aforementioned studies centered around single aspects of energy efficiency or environmental performance rather than integrated EEP measurements. A few researchers have investigated the integrated EEP by new DEA models. Wang, et al. [33], for example, used DEA window analysis to find that EEP is highest in the eastern area of China compared to other regions. Zhou and Wang [34] explored the energy and CO_2 emission performance for over 100 countries by using a new directional distance function (DDF). Zhou, et al. [35], Vlontzos, et al. [36], Meng, et al. [37], Geng, et al. [38], Wang and Zhao [39], and Perez, et al. [40] measured integrated EEP in their respective studies. Previous researchers have tended to focus on the regional or national level and lack of research down to the city level, though cities play an important role in environmental governance. Cities are responsible for 75-80% of global greenhouse emissions [41, 42]. Only a few researchers, e.g., Li, et al. [43], Yuan, et al. [44], Wang, et al. [45], Zhou, et al. [46], and Guo, et al. [47] have explored environmental performance at the city level.

In the present study, we extended the extant research in two main aspects. In terms of methodology, we propose an additive DEA model combined with a slack-based measure and non-radial directional distance function as first developed by Färe and Grosskopf [48]. The Luenberger productivity index with an additive structure is used to measure changes in productivity (which differs from the Malmquist index with multiplicative structure). We established a biennial Luenberger index extended from biennial Malmquist index proposed by Pastor, et al. [49] to avoid infeasibility solution of DEA. In terms of indicator selection, we properly account for multi-undesirable outputs and compare these sub-performances. We also use the natural breaks method to identify break points by picking the class breaks which maintain the greatest similarity in one class but maximize the difference among different classes. Geographical location has a marked effect on the emission abatement potential, so we alter the traditional regression to geographically weighted regression (GWR) to allow our estimated coefficients of influencing factors to vary by location. The remainder of this paper is organized as follows. Section 2 presents the non-radial DEA model, decomposition method, and GWR estimation. Section 3 explains our data sources and presents our results with discussion. Section 4 summarizes our main conclusions.

2. Methodology

2.1. Biennial Energy and Environmental Production Technology

Consider a production process with the vectors of non-energy inputs ($\mathbf{x}$), such as labor and capital input, and the vectors of energy inputs ($\mathbf{e}$) to produce the vectors of desirable outputs ($\mathbf{y}$) and undesirable outputs ($\mathbf{b}$). The corresponding production set, called the energy and environmental production technology set, is:

$$\mathbf{T} = \left\{ (\mathbf{x}, \mathbf{e}, \mathbf{y}, \mathbf{b}) : (\mathbf{x}, \mathbf{e}) \text{ can produce } (\mathbf{y}, \mathbf{b}) \right\} \quad (1)$$

In the energy and environmental production technology set $\mathbf{T}$, inputs and desirable outputs are assumed to be strongly disposable. $\mathbf{T}$ satisfies two additional assumptions proposed by Färe,

Preprints (www.preprints.org) | NOT PEER-REVIEWED | Posted: 6 June 2018 doi:10.20944/preprints201806.0080.v1

Peer-reviewed version available at Sustainability 2018, 10, 2303; doi:10.3390/su10072303

Grosskopf, Lovell and Pasurka [19] to model a production technology that includes both desirable and undesirable outputs.

(1) Weak disposability assumption: If $(\mathbf{x},\mathbf{e},\mathbf{y},\mathbf{b}) \in \mathbf{T}$ and $0 \le \theta \le 1$, then $(\mathbf{x},\mathbf{e},\theta\mathbf{y},\theta\mathbf{b}) \in \mathbf{T}$. It means that we can not reduce undesirable outputs alone while keeping the desirable outputs constant. In practice, it is feasible to reduce the desirable outputs and undesirable outputs at the same time; undesirable outputs can be abated at the cost of a decrease in desirable output.

(2) Null-jointness assumption: If $(\mathbf{x},\mathbf{e},\mathbf{y},\mathbf{b}) \in \mathbf{T}$ and $\mathbf{b} = \mathbf{0}$, then $\mathbf{y} = \mathbf{0}$. Production must cease entirely in order to fully eliminate undesirable outputs.

It is unlikely to find a concrete production function which depicts the energy and environmental production technology set $\mathbf{T}$. Here, we use nonparametric DEA technology to approximately represent $\mathbf{T}$ with piecewise linear combinations of the observed data. On the assumption of constant returns to scale (CRS), the energy and environmental production technology $\mathbf{T}$ can be estimated as follows:

$$\begin{aligned}\hat{\mathbf{T}} = \{(\mathbf{x},\mathbf{e},\mathbf{y},\mathbf{b}) : & \sum_{k=1}^{K}\lambda_k x_{mk} \le x_{mo},\ m=1,2,\cdots,M;\ \sum_{k=1}^{K}\lambda_k e_{qk} \le e_{qo},\quad q=1,2,\cdots,Q \\ & \sum_{k=1}^{K}\lambda_k y_{nk} \ge y_{no},\ n=1,2,\cdots,N;\ \sum_{k=1}^{K}\lambda_k b_{jk} = b_{jo},\quad j=1,2,\cdots,J \\ & \lambda_k \ge 0,\quad k=1,2,\cdots,K\}\end{aligned} \tag{2}$$

where λ_k is the intensity variable that ensures the technology set $\mathbf{T}$ is bounded and closed. The first three inequality constraints indicate the strong disposability on inputs and desirable outputs. To ensure technology set $\mathbf{T}$ satisfies the weak disposability and null-jointness assumptions, the equality constraint is imposed on undesirable outputs.

Technology is generally stable in the short run, so we neglect technological changes from period "t" to "t+1", and combine technology set $\mathbf{T^t}$ and $\mathbf{T^{t+1}}$ together as $\mathbf{T^B} = \mathbf{T^t} \cup \mathbf{T^{t+1}}$, namely, biennial energy and environmental technology, which represents the comprehensive technology shared by periods "t" and "t+1". In order to estimate $\mathbf{T^B}$, we use observations from periods "t" and "t+1" to construct the biennial energy and environmental DEA technology $\hat{\mathbf{T}}^{\mathrm{B}}$ as-formed by following linear constraints:

$$\begin{aligned}\hat{\mathbf{T}}^{\mathbf{B}} = \{(\mathbf{x},\mathbf{e},\mathbf{y},\mathbf{b}) : & \sum_{k=1}^{K}\lambda_k^{t+1}x_{mk}^{t+1} + \sum_{k=1}^{K}\lambda_k^{t}x_{mk}^{t} \le x_{mo}\quad m=1,2,\cdots,M \\ & \sum_{k=1}^{K}\lambda_k^{t+1}e_{qk}^{t+1} + \sum_{k=1}^{K}\lambda_k^{t}e_{qk}^{t} \le \mathrm{e}_{qo}\quad \mathrm{q}=1,2,\cdots,Q \\ & \sum_{k=1}^{K}\lambda_k^{t+1}y_{nk}^{t+1} + \sum_{k=1}^{K}\lambda_k^{t}y_{nk}^{t} \ge y_{no}\quad n=1,2,\cdots,N \\ & \sum_{k=1}^{K}\lambda_k^{t+1}b_{jk}^{t+1} + \sum_{k=1}^{K}\lambda_k^{t}b_{jk}^{t} = b_{jo}\quad j=1,2,\cdots,J \\ & \lambda_k^{t} \ge 0;\ \lambda_k^{t+1} \ge 0;\ k=1,2,\cdots,K\end{aligned} \tag{3}$$

Model (3) can avoid infeasible solutions to the DEA model when dealing with cross-period data. Based on $\hat{\mathbf{T}}^{\mathrm{B}}$, we propose a biennial Luenberger productivity index derived from the concept of the biennial Malmquist productivity index [49].

2.2. Biennial Luenberger Energy and Environmental Performance Index

The Luenberger productivity index deduced by directional distance function (DDF) was first proposed by Chambers, et al. [50]. The DDF allowing the simultaneous evaluation of input contractions and output expansions can be defined as:

$$\overrightarrow{D}\left[\mathbf{x},\mathbf{e},\mathbf{y},\mathbf{b};\mathbf{g}=\left(-\mathbf{g}_{\mathbf{x}},-\mathbf{g}_{\mathbf{e}},\mathbf{g}_{\mathbf{y}},-\mathbf{g}_{\mathbf{b}}\right)\right] = \sup\left[\beta \middle| \left(\mathbf{x}-\beta\mathbf{g}_{\mathbf{x}},\mathbf{e}-\beta\mathbf{g}_{\mathbf{e}},\mathbf{y}+\beta\mathbf{g}_{\mathbf{y}},\mathbf{b}-\beta\mathbf{g}_{\mathbf{b}}\right) \in \mathbf{T}\right] \tag{4}$$

Preprints (www.preprints.org) | NOT PEER-REVIEWED | Posted: 6 June 2018 doi:10.20944/preprints201806.0080.v1

Peer-reviewed version available at Sustainability 2018, 10, 2303; doi:10.3390/su10072303

where $\mathbf{g}=(-\mathbf{g_x},-\mathbf{g_e},\mathbf{g_y},-\mathbf{g_b})$ is the directional vector.

Based on the Luenberger productivity index, the EEP change can be decomposed into energy and environmental technical efficiency change (catch-up effect) and energy and environmental technological change (frontier-shift effect). For the biennial periods "t" and "t+1", we first select technology in the period "t" as the benchmark and then examine the EEP change by the difference in DDFs from periods "t" to "t+1" referred to technology set $\mathbf{T^t}$. Energy and environmental performance index (EEPI) used to measure the EEP change is defined as follows:

$$EEPI^{t,t+1}\left(\mathbf{x}^t,\mathbf{e}^t,\mathbf{y}^t,\mathbf{b}^t,\mathbf{x}^{t+1},\mathbf{e}^{t+1},\mathbf{y}^{t+1},\mathbf{b}^{t+1};\mathbf{g}\right)=\vec{D}^t\left(\mathbf{x}^t,\mathbf{e}^t,\mathbf{y}^t,\mathbf{b}^t;\mathbf{g}\right)-\vec{D}^t\left(\mathbf{x}^{t+1},\mathbf{e}^{t+1},\mathbf{y}^{t+1},\mathbf{b}^{t+1};\mathbf{g}\right) \tag{5}$$

Similarly, EEPI can be defined with regard to the technology of the period "t+1":

$$EEPI^{t,t+1}\left(\mathbf{x}^t,\mathbf{e}^t,\mathbf{y}^t,\mathbf{b}^t,\mathbf{x}^{t+1},\mathbf{e}^{t+1},\mathbf{y}^{t+1},\mathbf{b}^{t+1};\mathbf{g}\right)=\vec{D}^{t+1}\left(\mathbf{x}^t,\mathbf{e}^t,\mathbf{y}^t,\mathbf{b}^t,\mathbf{g}\right)-\vec{D}^{t+1}\left(\mathbf{x}^{t+1},\mathbf{e}^{t+1},\mathbf{y}^{t+1},\mathbf{b}^{t+1};\mathbf{g}\right) \tag{6}$$

We compute the simple arithmetic mean of Eq. (5) and (6) to eliminate the bias derived from arbitrary period selection:

$$\begin{aligned}&EEPI^{t,t+1}\left(\mathbf{x}^t,\mathbf{e}^t,\mathbf{y}^t,\mathbf{b}^t,\mathbf{x}^{t+1},\mathbf{e}^{t+1},\mathbf{y}^{t+1},\mathbf{b}^{t+1};\mathbf{g}\right)\\&=\frac{1}{2}\left\{\begin{array}{l}\left[\vec{D}^t\left(\mathbf{x}^t,\mathbf{e}^t,\mathbf{y}^t,\mathbf{b}^t;\mathbf{g}\right)-\vec{D}^t\left(\mathbf{x}^{t+1},\mathbf{e}^{t+1},\mathbf{y}^{t+1},\mathbf{b}^{t+1};\mathbf{g}\right)\right]\\+\left[\vec{D}^{t+1}\left(\mathbf{x}^t,\mathbf{e}^t,\mathbf{y}^t,\mathbf{b}^t,\mathbf{g}\right)-\vec{D}^{t+1}\left(\mathbf{x}^{t+1},\mathbf{e}^{t+1},\mathbf{y}^{t+1},\mathbf{b}^{t+1},\mathbf{g}\right)\right]\end{array}\right\}\end{aligned} \tag{7}$$

The energy and environmental technical efficiency is defined by the differences in DDFs from period "t" to "t+1" with respect to their own technologies; this reveals the change in distances of one observation in two periods "t" and "t+1" to the corresponding frontier of technologies "t" and "t+1" respectively.

$$effch^{t,t+1}\left[\mathbf{x}^t,\mathbf{e}^t,\mathbf{y}^t,\mathbf{b}^t,\mathbf{x}^{t+1},\mathbf{e}^{t+1},\mathbf{y}^{t+1},\mathbf{b}^{t+1};\mathbf{g}\right]=\vec{D}^t\left(\mathbf{x}^t,\mathbf{e}^t,\mathbf{y}^t,\mathbf{b}^t;\mathbf{g}\right)-\vec{D}^{t+1}\left(\mathbf{x}^{t+1},\mathbf{e}^{t+1},\mathbf{y}^{t+1},\mathbf{b}^{t+1};\mathbf{g}\right) \tag{8}$$

The energy and environmental technological change can be measured by comparing the distance from one observed data point in the period "t" to the frontier of technology set of periods "t" and "t+1" respectively, which measures the distance between two technologies "t" and "t+1".

$$techch^{t,t+1}(\mathbf{x}^t,\mathbf{e}^t,\mathbf{y}^t,\mathbf{b}^t,\mathbf{x}^{t+1},\mathbf{e}^{t+1},\mathbf{y}^{t+1},\mathbf{b}^{t+1};\mathbf{g})=\vec{D}^{t+1}(\mathbf{x}^t,\mathbf{e}^t,\mathbf{y}^t,\mathbf{b}^t;\mathbf{g})-\vec{D}^t(\mathbf{x}^t,\mathbf{e}^t,\mathbf{y}^t,\mathbf{b}^t;\mathbf{g}) \tag{9}$$

Similar to Eq. (9), the energy and environmental technological change can be defined by comparing one observed data point in the period "t+1" to the technology of period "t" and "t+1"respectively:

$$techch^{t,t+1}(\mathbf{x}^t,\mathbf{e}^t,\mathbf{y}^t,\mathbf{b}^t,\mathbf{x}^{t+1},\mathbf{e}^{t+1},\mathbf{y}^{t+1},\mathbf{b}^{t+1};\mathbf{g})=\vec{D}^{t+1}(\mathbf{x}^{t+1},\mathbf{e}^{t+1},\mathbf{y}^{t+1},\mathbf{b}^{t+1};\mathbf{g})-\vec{D}^t(\mathbf{x}^{t+1},\mathbf{e}^{t+1},\mathbf{y}^{t+1},\mathbf{b}^{t+1};\mathbf{g}) \tag{10}$$

We also compute the simple arithmetic mean of Eqs. (9) and (10) to eliminate the bias of period selection:

$$\begin{aligned}&techch^{t,t+1}\left(\mathbf{x}^t,\mathbf{e}^t,\mathbf{y}^t,\mathbf{b}^t,\mathbf{x}^{t+1},\mathbf{e}^{t+1},\mathbf{y}^{t+1},\mathbf{b}^{t+1};\mathbf{g}\right)\\&=\frac{1}{2}\left\{\begin{array}{l}\left[\vec{D}^{t+1}\left(\mathbf{x}^t,\mathbf{e}^t,\mathbf{y}^t,\mathbf{b}^t;\mathbf{g}\right)-\vec{D}^t\left(\mathbf{x}^t,\mathbf{e}^t,\mathbf{y}^t,\mathbf{b}^t;\mathbf{g}\right)\right]\\+\left[\vec{D}^{t+1}\left(\mathbf{x}^{t+1},\mathbf{e}^{t+1},\mathbf{y}^{t+1},\mathbf{b}^{t+1};\mathbf{g}\right)-\vec{D}^t\left(\mathbf{x}^{t+1},\mathbf{e}^{t+1},\mathbf{y}^{t+1},\mathbf{b}^{t+1};\mathbf{g}\right)\right]\end{array}\right\}\end{aligned} \tag{11}$$

Equations (7), (8), and (11) can be combined into a comprehensive equation which reflects the additive structure of the Luenberger productivity index:

$$EEPI^{t,t+1}=effch^{t,t+1}+techch^{t,t+1} \tag{12}$$

Per the definition of $\vec{D}^t$ or $\vec{D}^{t+1}$, the biennial DDF based on $\mathbf{T^B}$ instead of $\mathbf{T}$ is:

Preprints (www.preprints.org) | NOT PEER-REVIEWED | Posted: 6 June 2018 doi:10.20944/preprints201806.0080.v1

Peer-reviewed version available at Sustainability 2018, 10, 2303; doi:10.3390/su10072303

$$\vec{D}^{\mathbf{B}}\left[\mathbf{x},\mathbf{e},\mathbf{y},\mathbf{b};\mathbf{g}=\left(-\mathbf{g}_{\mathbf{x}},-\mathbf{g}_{\mathbf{e}},\mathbf{g}_{\mathbf{y}},-\mathbf{g}_{\mathbf{b}}\right)\right]=\sup\left[\beta\left|\left(\mathbf{x}-\beta\mathbf{g}_{\mathbf{x}},\mathbf{e}-\beta\mathbf{g}_{\mathbf{e}},\mathbf{y}+\beta\mathbf{g}_{\mathbf{y}},\mathbf{b}-\beta\mathbf{g}_{\mathbf{b}}\right)\in\mathbf{T}^{\mathbf{B}}\right.\right] \quad (13)$$

Similar to the definition of above Luenberger productivity index, the biennial Luenberger productivity index has two components:

$$EEPI_{B}^{t,t+1}\left(\mathbf{x}^{t},\mathbf{e}^{t},\mathbf{y}^{t},\mathbf{b}^{t},\mathbf{x}^{t+1},\mathbf{e}^{t+1},\mathbf{y}^{t+1},\mathbf{b}^{t+1};\mathbf{g}\right)=\vec{D}^{B}\left(\mathbf{x}^{t},\mathbf{e}^{t},\mathbf{y}^{t},\mathbf{b}^{t};\mathbf{g}\right)-\vec{D}^{B}\left(\mathbf{x}^{t+1},\mathbf{e}^{t+1},\mathbf{y}^{t+1},\mathbf{b}^{t+1};\mathbf{g}\right) \quad (14)$$

$$effch_{B}^{t,t+1}\left(\mathbf{x}^{t},\mathbf{e}^{t},\mathbf{y}^{t},\mathbf{b}^{t},\mathbf{x}^{t+1},\mathbf{e}^{t+1},\mathbf{y}^{t+1},\mathbf{b}^{t+1};\mathbf{g}\right)=\vec{D}^{t}\left(\mathbf{x}^{t},\mathbf{e}^{t},\mathbf{y}^{t},\mathbf{b}^{t};\mathbf{g}\right)-\vec{D}^{t+1}\left(\mathbf{x}^{t+1},\mathbf{e}^{t+1},\mathbf{y}^{t+1},\mathbf{b}^{t+1};\mathbf{g}\right) \quad (15)$$

$$\begin{aligned}techch_{B}^{t,t+1}\left(\mathbf{x}^{t},\mathbf{e}^{t},\mathbf{y}^{t},\mathbf{b}^{t},\mathbf{x}^{t+1},\mathbf{e}^{t+1},\mathbf{y}^{t+1},\mathbf{b}^{t+1};\mathbf{g}\right)=&\left[\vec{D}^{B}\left(\mathbf{x}^{t},\mathbf{e}^{t},\mathbf{y}^{t},\mathbf{b}^{t};\mathbf{g}\right)-\vec{D}^{t}\left(\mathbf{x}^{t},\mathbf{e}^{t},\mathbf{y}^{t},\mathbf{b}^{t};\mathbf{g}\right)\right]\\&-\left[\vec{D}^{B}\left(\mathbf{x}^{t+1},\mathbf{e}^{t+1},\mathbf{y}^{t+1},\mathbf{b}^{t+1};\mathbf{g}\right)-\vec{D}^{t+1}\left(\mathbf{x}^{t+1},\mathbf{e}^{t+1},\mathbf{y}^{t+1},\mathbf{b}^{t+1};\mathbf{g}\right)\right]\end{aligned} \quad (16)$$

$$EEPI_{B}^{t,t+1}=effch_{B}^{t,t+1}+techch_{B}^{t,t+1} \quad (17)$$

2.3. Energy and Environmental Performance Measurement with Non-radial DEA Model

Based on the definition of DDF (Eqs. (4), (13)) and estimated technology set of $\hat{\mathbf{T}}$ and $\hat{\mathbf{T}}^{\mathbf{B}}$ (Models (2), (3)), the radial DDF can be estimated by the following DEA models:

$$\begin{aligned}&\hat{\vec{D}}^{t}\left[\mathbf{x},\mathbf{e},\mathbf{y},\mathbf{b};\mathbf{g}=\left(-\mathbf{x},-\mathbf{e},\mathbf{y},-\mathbf{b}\right)\right]=\max\beta\\&\sum_{k=1}^{K}\lambda_{k}^{t}x_{mk}^{t}\le(1-\beta)x_{mo}\quad m=1,2,\cdots,M\\&\sum_{k=1}^{K}\lambda_{k}^{t}e_{qk}^{t}\le(1-\beta)e_{qo}\quad q=1,2,\cdots,Q\\&\sum_{k=1}^{K}\lambda_{k}^{t}y_{nk}^{t}\ge(1+\beta)y_{no}\quad n=1,2,\cdots,N\\&\sum_{k=1}^{K}\lambda_{k}^{t}b_{jk}^{t}=(1-\beta)b_{jo}\quad j=1,2,\cdots,J\\&\lambda_{k}^{t}\ge0;\qquad k=1,2,\cdots,K\end{aligned} \quad (18)$$

$$\begin{aligned}&\hat{\vec{D}}^{\mathbf{B}}\left[\mathbf{x},\mathbf{e},\mathbf{y},\mathbf{b};\mathbf{g}=\left(-\mathbf{x},-\mathbf{e},\mathbf{y},-\mathbf{b}\right)\right]=\max\beta\\&\sum_{k=1}^{K}\lambda_{k}^{t+1}x_{mk}^{t+1}+\sum_{k=1}^{K}\lambda_{k}^{t}x_{mk}^{t}\le(1-\beta)x_{mo}\quad m=1,2,\cdots,M\\&\sum_{k=1}^{K}\lambda_{k}^{t+1}e_{qk}^{t+1}+\sum_{k=1}^{K}\lambda_{k}^{t}e_{qk}^{t}\le(1-\beta)e_{qo}\quad q=1,2,\cdots,Q\\&\sum_{k=1}^{K}\lambda_{k}^{t+1}y_{nk}^{t+1}+\sum_{k=1}^{K}\lambda_{k}^{t}y_{nk}^{t}\ge(1+\beta)y_{no}\quad n=1,2,\cdots,N\\&\sum_{k=1}^{K}\lambda_{k}^{t+1}b_{jk}^{t+1}+\sum_{k=1}^{K}\lambda_{k}^{t}b_{jk}^{t}=(1-\beta)b_{jo}\quad j=1,2,\cdots,J\\&\lambda_{k}^{t}\ge0;\ \lambda_{k}^{t+1}\ge0;\ k=1,2,\cdots,K\end{aligned} \quad (19)$$

Traditional and biennial DDFs can be computed by Models (18) and (19), respectively. β denotes the slack ratio (adjustment rate) or "inefficiency score". If $\beta=0$, then the corresponding DMU is considered to be efficient and with no improvement potential. $\beta>0$ indicates that the corresponding DMU is inefficient and has not yet achieved the relative optimization. Models (18) and (19) are regarded as radial DDFs with the same adjustment rate.

The radial DDF gives the same contraction (expansion) to all the inputs (outputs) and thus may have weak technical efficiency. Increasing desirable outputs and decreasing inputs and undesirable outputs can be further achieved under the current technical conditions, i.e., the radial DDF overestimates the efficiency. The non-radial DDF can further identify potential in increasing inputs

and decreasing outputs, so we use a non-radial DDF model to measure EEP here. Mathematically, traditional and biennial radial DDFs can be improved by the following DEA models:

$$
\begin{aligned}
&\widehat{D}^{t}\left[\mathbf{x},\mathbf{e},\mathbf{y},\mathbf{b};\mathbf{g}=(\mathbf{-x},\mathbf{-e},\mathbf{y},\mathbf{-b})\right]\\
&=\max\frac{1}{4}\left(\frac{1}{M}\sum_{m=1}^{M}\beta_m+\frac{1}{Q}\sum_{q=1}^{Q}\beta_q+\frac{1}{N}\sum_{n=1}^{N}\beta_n+\frac{1}{J}\sum_{j=1}^{J}\beta_j\right)\\
&\sum_{k=1}^{K}\lambda_k^t x_{mk}^t\le(1-\beta_m)x_{mo}\quad m=1,2,\cdots,M\\
&\sum_{k=1}^{K}\lambda_k^t e_{qk}^t\le(1-\beta_q)e_{qo}\quad q=1,2,\cdots,Q\\
&\sum_{k=1}^{K}\lambda_k^t y_{nk}^t\ge(1+\beta_n)y_{no}\quad n=1,2,\cdots,N\\
&\sum_{k=1}^{K}\lambda_k^t b_{jk}^t=(1-\beta_j)b_{jo}\quad j=1,2,\cdots,J\\
&\lambda_k^t\ge 0;\qquad k=1,2,\cdots,K
\end{aligned}
\tag{20}
$$

$$
\begin{aligned}
&\widehat{D}^{\mathbf{B}}\left[\mathbf{x},\mathbf{e},\mathbf{y},\mathbf{b};\mathbf{g}=(\mathbf{-x},\mathbf{-e},\mathbf{y},\mathbf{-b})\right]\\
&=\max\frac{1}{4}\left(\frac{1}{M}\sum_{m=1}^{M}\beta_m+\frac{1}{Q}\sum_{q=1}^{Q}\beta_q+\frac{1}{N}\sum_{n=1}^{N}\beta_n+\frac{1}{J}\sum_{j=1}^{J}\beta_j\right)\\
&\sum_{k=1}^{K}\lambda_k^{t+1}x_{mk}^{t+1}+\sum_{k=1}^{K}\lambda_k^t x_{mk}^t\le(1-\beta_m)x_{mo}\ m=1,2,\cdots,M\\
&\sum_{k=1}^{K}\lambda_k^{t+1}e_{qk}^{t+1}+\sum_{k=1}^{K}\lambda_k^t e_{qk}^t\le(1-\beta_q)\mathrm{e}_{qo}\quad q=1,2,\cdots,Q\\
&\sum_{k=1}^{K}\lambda_k^{t+1}y_{nk}^{t+1}+\sum_{k=1}^{K}\lambda_k^t y_{nk}^t\ge(1+\beta_n)y_{no}\quad n=1,2,\cdots,N\\
&\sum_{k=1}^{K}\lambda_k^{t+1}b_{jk}^{t+1}+\sum_{k=1}^{K}\lambda_k^t b_{jk}^t=(1-\beta_j)b_{jo}\quad j=1,2,\cdots,J\\
&\lambda_k^t\ge 0;\ \lambda_k^{t+1}\ge 0;\ k=1,2,\cdots,K
\end{aligned}
\tag{21}
$$

In Models (20) and (21), β_m , β_q , β_n, or β_j represents the ratio of the slack to a non-energy input, energy input, desirable output, and undesirable output respectively. If $\beta_m=\beta_q=\beta_n=\beta_j$, Models (20) and (21) are converted into Models (18) and (19). The non-radial DDF allows us to exploit slacks more exhaustively with stronger discrimination power than the radial DDF [51]. We mainly focused on energy conservation and pollution reduction in this study, so the directional vector is set to $\mathbf{g}=(\mathbf{0},-\mathbf{e},\mathbf{0},-\mathbf{b})$ here. The DDF we used can be calculated by the following DEA linear programming models:

$$
\begin{aligned}
&\widehat{D}^{t}\left[\mathbf{x},\mathbf{e},\mathbf{y},\mathbf{b};\mathbf{g}=(\mathbf{0},\mathbf{-e},\mathbf{0},\mathbf{-b})\right]\\
&=\max\frac{1}{2}\left(\frac{1}{Q}\sum_{q=1}^{Q}\beta_q+\frac{1}{J}\sum_{j=1}^{J}\beta_j\right)\\
&\sum_{k=1}^{K}\lambda_k^t x_{mk}^t\le x_{mo}\qquad m=1,2,\cdots,M\\
&\sum_{k=1}^{K}\lambda_k^t e_{qk}^t\le(1-\beta_q)e_{qo}\quad q=1,2,\cdots,Q\\
&\sum_{k=1}^{K}\lambda_k^t y_{nk}^t\ge y_{no}\qquad n=1,2,\cdots,N\\
&\sum_{k=1}^{K}\lambda_k^t b_{jk}^t=(1-\beta_j)b_{jo}\quad j=1,2,\cdots,J\\
&\lambda_k^t\ge 0;\qquad k=1,2,\cdots,K
\end{aligned}
\tag{22}
$$

$$
\begin{aligned}
&\widehat{D}^{\mathbf{B}}\left[\mathbf{x},\mathbf{e},\mathbf{y},\mathbf{b};\mathbf{g}=(\mathbf{0},-\mathbf{e},\mathbf{0},-\mathbf{b})\right] \\
&=\max\frac{1}{2}\left(\frac{1}{Q}\sum_{q=1}^{Q}\beta_q+\frac{1}{J}\sum_{j=1}^{J}\beta_j\right) \\
&\sum_{k=1}^{K}\lambda_k^{t+1}x_{mk}^{t+1}+\sum_{k=1}^{K}\lambda_k^{t}x_{mk}^{t}\le x_{mo} \qquad m=1,2,\cdots,M \\
&\sum_{k=1}^{K}\lambda_k^{t+1}e_{qk}^{t+1}+\sum_{k=1}^{K}\lambda_k^{t}e_{qk}^{t}\le(1-\beta_q)\mathrm{e}_{qo} \quad \mathrm{q}=1,2,\cdots,\ Q \\
&\sum_{k=1}^{K}\lambda_k^{t+1}y_{nk}^{t+1}+\sum_{k=1}^{K}\lambda_k^{t}y_{nk}^{t}\ge y_{no} \qquad n=1,2,\cdots,\ N \\
&\sum_{k=1}^{K}\lambda_k^{t+1}b_{jk}^{t+1}+\sum_{k=1}^{K}\lambda_k^{t}b_{jk}^{t}=(1-\beta_j)b_{jo} \quad j=1,2,\cdots,\ J \\
&\lambda_k^{t}\ge 0;\ \lambda_k^{t+1}\ge 0;\ k=1,2,\cdots,K
\end{aligned}
\tag{23}
$$

In Models (22) and (23), β_q and β_j represent the ratios of energy conservation and emission abatement, respectively. $\vec{D}^t(\mathbf{x}^t,\mathbf{e}^t,\mathbf{y}^t,\mathbf{b}^t;\mathbf{g})$ represents the energy and environmental inefficiency, so we can calculate EEP by $1-\vec{D}^t(\mathbf{x}^t,\mathbf{e}^t,\mathbf{y}^t,\mathbf{b}^t;\mathbf{g})$.

If input-output combination $(\mathbf{x},\mathbf{e},\mathbf{y},\mathbf{b})$ is observed in the period "t" for two technologies in the period "t" and "t+1" respectively, we can estimate $\vec{D}^t(\mathbf{x}^t,\mathbf{e}^t,\mathbf{y}^t,\mathbf{b}^t;\mathbf{g})$ and $\vec{D}^{t+1}(\mathbf{x}^t,\mathbf{e}^t,\mathbf{y}^t,\mathbf{b}^t;\mathbf{g})$ with Model (22). We can estimate $\vec{D}^t(\mathbf{x}^{t+1},\mathbf{e}^{t+1},\mathbf{y}^{t+1},\mathbf{b}^{t+1};\mathbf{g})$ and $\vec{D}^{t+1}(\mathbf{x}^{t+1},\mathbf{e}^{t+1},\mathbf{y}^{t+1},\mathbf{b}^{t+1};\mathbf{g})$ similarly. We can also estimate $\vec{D}^B(\mathbf{x}^t,\mathbf{e}^t,\mathbf{y}^t,\mathbf{b}^t;\mathbf{g})$ and $\vec{D}^B(\mathbf{x}^{t+1},\mathbf{e}^{t+1},\mathbf{y}^{t+1},\mathbf{b}^{t+1};\mathbf{g})$ by employing Model (23) with production activity $(\mathbf{x},\mathbf{e},\mathbf{y},\mathbf{b})$ observed in the period "t" and "t+1" respectively.

To calculate the Luenberger EEPI which represents the EEP change, we need to calculate six DDFs (activities in "t" and "t+1" refer to technologies in the period "t", "t+1" and pooled respectively) by Models (22) and (23). Given that different undesirable output structures impact the EEP, a non-radial efficiency measure can help us identify specific effects and contributions of energy factor and specific undesirable outputs. The total EEPI can be further decomposed into specific EEPIs to analyze the contributions of specific undesirable outputs and energy inputs on total EEPI.

2.4. Exploratory Spatial Data Analysis- Moran's Index

The sample data we used contains abundant spatial information, so we sought to consider the spatial effects on EEP among different cities. We did so by applying Exploratory Spatial Data Analysis (ESDA) to describe the spatial distribution of the EEP. We used Moran's I statistic to measure the spatial correlation at the city level, including global spatial correlation and local spatial correlation [52].

(1) Global Moran's I statistics

The global Moran's I statistics reflect the similarity of attributes with their neighborhoods:

$$
Moran's\ I_g=\frac{\sum_{i=1}^{n}\sum_{j=1}^{n}w_{ij}(Y_i-\bar{Y})(Y_j-\bar{Y})}{S^2\sum_{i=1}^{n}\sum_{j=1}^{n}w_{ij}} \tag{24}
$$

where Y_i represents the observed value in the ith city; n represents the number of the cities; w_{ij} represents the spatial weight matrix which reflects the spatial adjacent relationship in the ith and jth cities. Global Moran's I ranges from -1 to 1: value less than 0 represents a negative correlation, 0 represents an uncorrelated relationship, and greater than 0 represents a positive correlation. As the global Moran's I moves towards -1, the spatial differences among cities become more obvious. If the obtained value of global Moran's I is near to 1, there are more intimate relations (e.g., high-value clusters or low-value clusters) among cities.

(2) Local Moran's I statistics

Preprints (www.preprints.org) | NOT PEER-REVIEWED | Posted: 6 June 2018 doi:10.20944/preprints201806.0080.v1

Peer-reviewed version available at Sustainability 2018, 10, 2303; doi:10.3390/su10072303

$$I_i = \frac{(x_i - \bar{x})}{S^2} \sum_j w_{ij}(x_j - \bar{x}) \tag{25}$$

If I_i is greater than 0, the ith spatial unit is similar to its neighbors (i.e., "high-high" or "low-low"); I_i, with a value lower than 0 represents dissimilarities to neighbors ("high-low" or "low-high"). We can also visually identify the high-value clusters and low-value clusters according to the map of local indicators of spatial association (LISA).

2.5. Geographically Weighted Regression Model

The spatial heterogeneity of our data means that explanatory variables have varying extent of influence on the explained variable in different areas. Under the traditional econometric regression model, regression parameters are same across whole regions and regional differences are neglected. The geographically weighted regression (GWR) model [53, 54], which takes the regional difference into account, allows regression parameters to change along with the geographical position. Regression parameters in GWR are a data set rather than a fixed coefficient. The GWR model can be derived as follows:

$$y_i = \beta_0(u_i, v_i) + \sum_{k=1}^{K} \beta_k(u_i, v_i) x_{ik} + \varepsilon_i \tag{26}$$

where vector y represents the explained variable; vector x represents explanatory variables; (u_i, v_i) is the space coordinate (longitude and latitude) in the area i. $\beta_k(u_i, v_i)$ is the regression parameter for the kth explanatory variable in the area i. ε_i is random error; we assume that $\varepsilon_i \sim N(0, \sigma^2)$ and $cov(\varepsilon_i, \varepsilon_j) = 0\ (i \neq j)$. To estimate regression parameters, we assign $w_1(u_i, v_i)$, $w_2(u_i, v_i), \cdots, w_n(u_i, v_i)$ for the area i to represent influences from all other areas [55]. According to the weighted least square method, we can then estimate the regression equation in (u_i, v_i) by minimizing the following equation:

$$\sum_{i=1}^{n} w_i(u_i, v_i)\left[y_i - \beta_0(u_i, v_i) - \beta_1(u_i, v_i)\mathrm{x}_{i1} - \cdots - \beta_K(u_i, v_i)x_{ik}\right]^2 \tag{27}$$

with

$$\mathbf{Y} = \begin{bmatrix} y_1 \\ y_2 \\ \vdots \\ y_n \end{bmatrix}, \mathbf{X} = \begin{bmatrix} x_{11} & x_{12} & \cdots & x_{1k} \\ x_{21} & x_{22} & \cdots & x_{2k} \\ \vdots & \vdots & \ddots & \vdots \\ x_{n1} & x_{n2} & x_3 & x_{nk} \end{bmatrix} = \begin{bmatrix} x_1' \\ x_2' \\ \vdots \\ x_n' \end{bmatrix}$$

$$\boldsymbol{\beta}(u_i, v_i) = \begin{bmatrix} \beta_1(u_i, v_i) \\ \beta_2(u_i, v_i) \\ \vdots \\ \beta_K(u_i, v_i) \end{bmatrix}, \mathbf{W}_{(u_i, v_i)} = \begin{bmatrix} w_{i1} & 0 & \cdots & 0 \\ 0 & w_{i2} & \cdots & 0 \\ \vdots & \vdots & \ddots & \vdots \\ 0 & 0 & \cdots & w_{ik} \end{bmatrix} \tag{28}$$

We can then derive $\hat{\beta}(u_i, v_i) = \left(\mathbf{X}^T \mathbf{W}_{(u_i, v_i)} \mathbf{X}\right)^{-1} \mathbf{X}^T \mathbf{W}_{(u_i, v_i)} \mathbf{Y}$. The spatial weighting function is the key to the above GWR model. Here, we use a Gaussian weighting function as the spatial weighting function [55].

3. Empirical Study

3.1. Data Source and Description

We initiated our analysis using a data set containing 283 cities in China over 2010-2014. Certain official statistics measurement criteria changed significantly in 2010, so we set the time period from

2010 to 2014 to maintain comparability across the data. We chose labor and capital as the two non-energy inputs. Labor is defined by the number of employees in a city's manufacturing industry excluding the employees working in the construction industry. To define capital, we referred to the total fixed assets and current assets at constant prices in 2010 [44]. We used the price indexes from corresponding provinces because fixed asset investment price indexes are not available at the city level. With regard to current assets, we adopted the consumer price index from the corresponding city to eliminate the influence of fluctuations in prices. We could not obtain total energy consumption in the industrial sector at the city level, so we chose the electricity consumption as an approximate substitution [46]. We used gross industrial output as the sole desirable output and adopted the ex-factory price index of industrial products to eliminate price fluctuations. The "undesirable outputs" referred to in this paper contain three specific pollutants: industrial wastewater, industrial sulfur dioxide (SO_2), and industrial soot. We also used the ratio of value added of the service industry in the city's GDP to analyze GWR. Data was collected from the China City Statistical Yearbook (2011-2015) [56] and China Provincial Statistical Yearbook (2011-2015) [57]. The descriptive statistics of inputs and outputs we applied to empirical analysis are shown in Table 1.

Table 1. Descriptive statistics of inputs and outputs in 2010-2014.

Index	Variable	Unit	Quantity	Mean	St.Dev	Min	Max
Non-energy input	Labor force	10 thousand persons	283×5	19.16	28.18	0.39	260.92
	Current assets	billion Yuan	283×5	116.27	196.44	0. 83	1808.43
	Fixed assets	billion Yuan	283×5	90.15	106.34	0.86	827.94
Energy input	Industrial electricity	100 million kWh	283×5	60.19	91.97	0.045	805.76
Desirable output	Gross industrial output	billion Yuan	283×5	310.31	423.71	1.53	3278.23
Undesirable output	Industrial wastewater	million tons	283×5	74.71	84.99	0.23	868.04
	Industrial sulfur dioxide	thousand tons	283×5	58.78	57.33	0.002	572.75
	Industrial soot	thousand tons	283×5	41.71	188.64	0.034	5168.81

3.2. Results and Discussion

3.2.1. Static Energy and Environmental Performance

3.2.1.1. Descriptive Statistics of Energy and Environmental Performance

We first compared the EEP and its decompositions consisting of energy, wastewater, SO_2, soot emission performance (sub-performance or sub-efficiency) at both national and regional levels. Our calculations of the mean, standard deviation, minimum value, and maximal value in the four areas involve five-year x cities' total performance and its decompositions (where x represents the number of cities in the corresponding area) encompassing both temporal and spatial dimensions. Table 2 shows the descriptive statistics of EEP for 283 cities in China in 2010-2014.

Table 2. Descriptive statistics of EEP and sub-performances.

Performance (efficiency)	Area	Quantity	Mean	St.Dev	Min	Max
Total	East	87×5	0.473	0.298	0.069	1.000
	China	**283×5**	**0.365**	**0.292**	**0.016**	**1.000**
	Central	99×5	0.362	0.282	0.031	1.000
	Northeast	33×5	0.272	0.236	0.025	1.000
	West	64×5	0.270	0.276	0.016	1.000
Energy	East	87×5	0.456	0.328	0.042	1.000
	Central	99×5	0.364	0.304	0.012	1.000
	China	**283×5**	**0.358**	**0.315**	**0.008**	**1.000**
	West	64×5	0.259	0.291	0.008	1.000
	Northeast	33×5	0.257	0.253	0.019	1.000
Wastewater	East	87×5	0.418	0.326	0.015	1.000
	China	**283×5**	**0.355**	**0.308**	**0.011**	**1.000**
	Central	99×5	0.347	0.303	0.038	1.000
	Northeast	33×5	0.333	0.283	0.024	1.000
	West	64×5	0.280	0.292	0.011	1.000
SO_2	East	87×5	0.481	0.330	0.037	1.000
	China	**283×5**	**0.358**	**0.321**	**0.007**	**1.000**
	Central	99×5	0.338	0.314	0.020	1.000
	Northeast	33×5	0.281	0.266	0.017	1.000
	West	64×5	0.264	0.303	0.007	1.000
Soot	East	87×5	0.572	0.336	0.014	1.000
	China	**283×5**	**0.403**	**0.339**	**0.014**	**1.000**
	Central	99×5	0.356	0.311	0.001	1.000
	West	64×5	0.299	0.311	0.004	1.000
	Northeast	33×5	0.246	0.267	0.014	1.000

3.2.1.2. Distribution Dynamic Analysis of Energy and Environmental Performance

We next tracked the EEP evolution for 283 cities in China via the distribution dynamics approach [58-60]. Each city's EEP and its decompositions were divided by 283 cities' yearly average levels to form the corresponding relative performance indicators. These indicators can then be used to estimate the kernel densities and stochastic kernels.

Figure 1 shows the distributions of kernel densities for the total performance and sub-performances. The distribution of total performance in 2010 is bimodal with more than 80% of cities' performance distributed around 0.5 times the average performance level and other cities' performance concentrated on 2.5 times level (possessed by the best performers). Most cities' total performances were below average in 2010, but a select few cities performed extremely well and formed a small convergence club led by best performers. In 2014, the distribution of total performance nearly reached around 0.5 times the average performance level; the small convergence club dispersed and members in it became smaller. The ergodic distribution indicates clear convergence to 0.5 times the average level and small convergence club would nearly disappear. Other kernel density plots for sub-performances indicate that: 1) energy performance features strong convergence to 0.5 times the average performance level; 2) small convergence clubs for environmental performances are more obvious than energy performance.

Preprints (www.preprints.org) | NOT PEER-REVIEWED | Posted: 6 June 2018 doi:10.20944/preprints201806.0080.v1

Peer-reviewed version available at Sustainability 2018, 10, 2303; doi:10.3390/su10072303

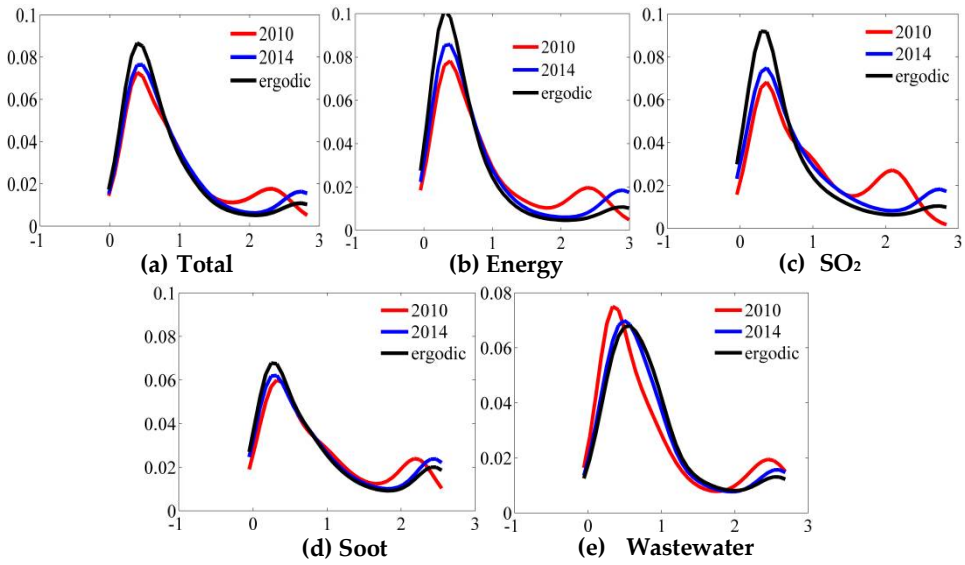

Figure 1. Distributions of total performance and sub-performances

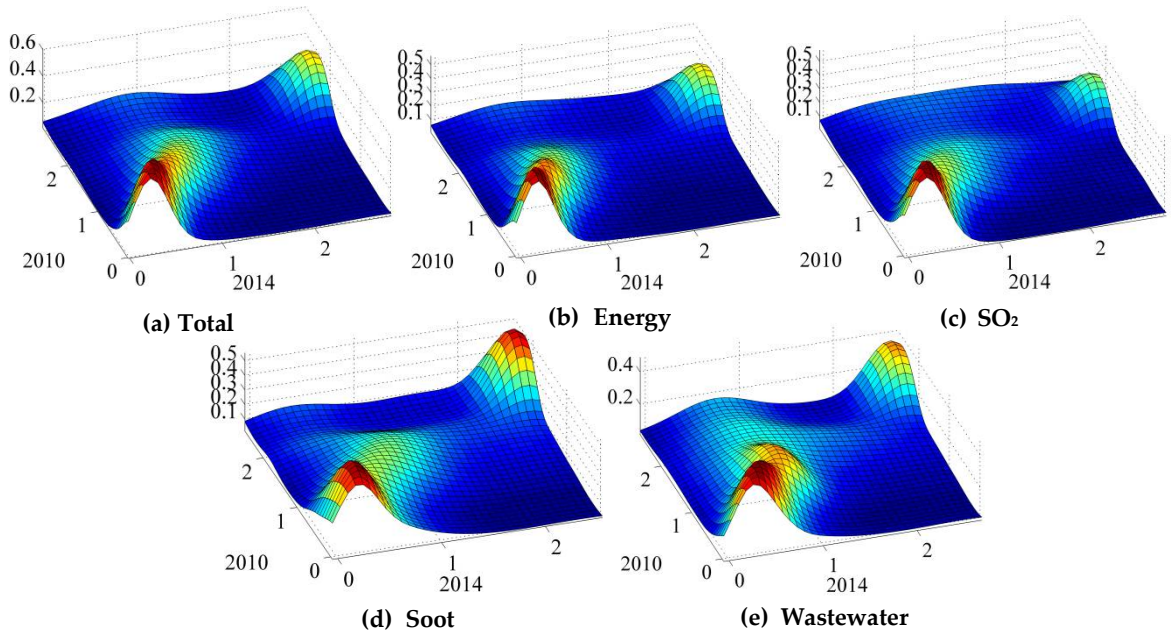

Figure 2. 3D surface of stochastic kernel plots for total and sub-performances

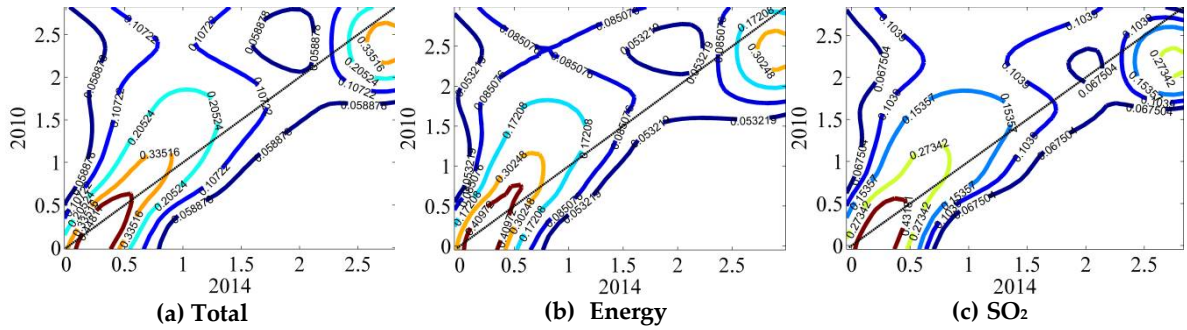

Preprints (www.preprints.org) | NOT PEER-REVIEWED | Posted: 6 June 2018 doi:10.20944/preprints201806.0080.v1

Peer-reviewed version available at Sustainability 2018, 10, 2303; doi:10.3390/su10072303

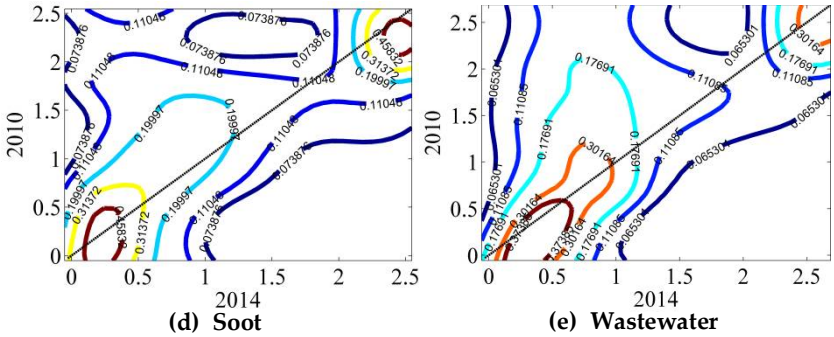

Figure 3. Contour stochastic kernel plots for total and sub-performances

As shown in the 3D stochastic kernel and 2D contour part plots (Figures 2-3), for cities with below-average levels in total performance and sub-performances, the transition probability generally moves counter-clockwise from the 45° diagonal – cities with relatively low EEP compared to the average level remarkably improved over the study period. Cities with above-average performance, conversely, can be divided into two groups: The first group, the small convergence club led by the best performers, remain near the 45° diagonal in the upper right-hand corner. In the second group, cities with high total performance and sub-performances gradually decrease in efficiency and converge to average levels.

3.2.1.3. Analysis of Best and Worst Performers

Identifying the best performers can provide good benchmarks for cities with lower efficiency in terms of energy conservation and emissions abatement. If EEP equals 1 ($D^t(\mathbf{x}^t, \mathbf{e}^t, \mathbf{y}^t, \mathbf{b}^t; \mathbf{g}) = 0$), i.e., the city was located in the production frontier for at least in one year between 2010 and 2014, the city is defined as a "best performer". As shown in Figure 4, the best performers are mainly located in Guangdong, Shandong, Jiangsu, Jiangxi, Sichuan, and Hainan provinces. The best performers possess advanced service industries, which generally consume few resources, or have high ecological quality. In Qingdao, Shenzhen, and Dongguan, for example, the ratio of service industry to GDP was 51.22%, 57.39%, and 52.14% in 2014, respectively. The service industry consumes relatively little energy though it does require a great deal of labor, capital, and technology. Besides, these developed cities with sufficient funding also can improve their energy conservation and abatement ability via technical innovation and advanced managerial experience. These cities consume less energy and emit less pollution while maximizing desirable outputs. Provinces such as Jiangxi, Sichuan, and Hainan have less developed economies but still exhibit high EEP due to natural endowments (high ecological quality) and economic support from tourism.

A city with EEP no more than 0.1 ($D^t(\mathbf{x}^t, \mathbf{e}^t, \mathbf{y}^t, \mathbf{b}^t; \mathbf{g}) > 0.9$) in all years of 2010-2014 is defined as a "worst performer". As shown in Figure 4, the worst performers are mainly distributed in Heilongjiang, Guangxi, Ningxia, and Shanxi provinces which are generally rich in coal or nonferrous metal resources. Cities like Datong (Shanxi), Shizuishan (Ningxia), Huainan (Anhui) and Hegang (Heilongjiang) are important coal bases of China. A great deal of pollutants are emitted by coal exploitation and processing. Other cities like Guigang (Guangxi) and Baise (also Guangxi) are important nonferrous metal bases of China. Nonferrous metallurgy likewise produces substantial air pollutants as well as mercury and chromium pollution.

Preprints (www.preprints.org) | NOT PEER-REVIEWED | Posted: 6 June 2018 doi:10.20944/preprints201806.0080.v1

Peer-reviewed version available at Sustainability 2018, 10, 2303; doi:10.3390/su10072303

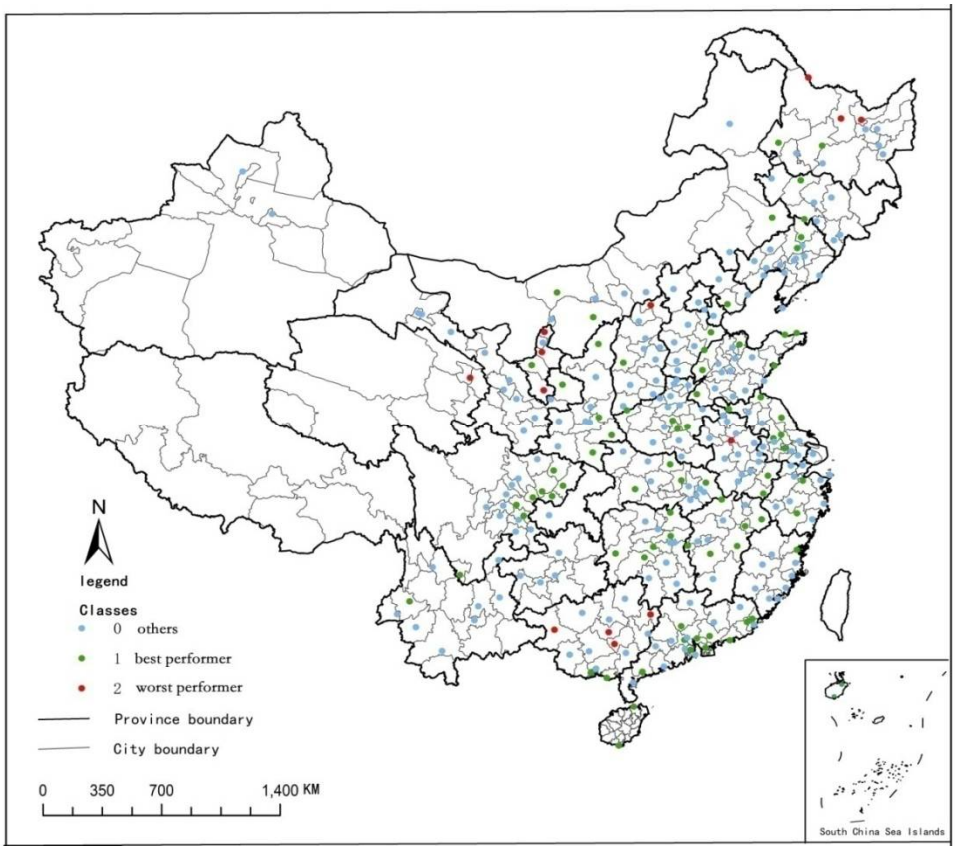

Figure 4. Distribution of best performers and worst performers

3.2.2. Analysis of Dynamic Changes in Energy and Environmental Performance

3.2.2.1. National Level

We examined dynamic changes in EEP and its decompositions by EEPI. We first calculated the average value at the country level involving a five-year span of 283 cities' total performance changes and decompositions over temporal and spatial dimensions. The average EEP change, technical efficiency change, and technological change are 2.38%, -1.57% and 3.95%, respectively (Table 3). That is to say, China made considerable progress in the energy conservation and emissions abatement in the study period. The Chinese government made great strides in environmental protection under the 12th five-year plan (FYP) (2011-2015), which focused on upgrading the industrial structure for low energy consumption and pollution reduction. Further, the manufacturing industry comprised 57.2% of GDP in 2010 but only 47.1% in 2014. Changes in technical efficiency continually declined with the exception of the period 2012-2013, whereas a slower and slower upward trend was observed in technological changes. In other words, EEP change is mainly driven by technological progress rather than technical efficiency improvement [11, 46, 61]. Government policies targeting the improvement of technical efficiency in the manufacturing sector may indeed enhance overall environmental performance.

Table 3. Arithmetic mean of EEPI and its decompositions for 283 cities

Index	2010-2011	2011-2012	2012-2013	2013-2014	average
$EEPI_{total}^{t,t+1}$	0.0004	0.0246	0.0634	0.0067	0.0238
$effch_{total}^{t,t+1}$	-0.0969	-0.0067	0.0579	-0.0172	-0.0157
$techch_{total}^{t,t+1}$	0.0973	0.0313	0.0055	0.0239	0.0395

Cities on the production frontier achieved rapid technological progress and made other cities more difficult to catch up with the production frontier. In other word, the decrease of technical efficiency is a relative deterioration caused by fast technological progress. The decline in technical efficiency is roughly consistent with observations previously made by Meng, Fan, Zhou and Zhou [61]. We further interpreted the deterioration of technical efficiency by assuming that a production activity with one energy input, one desirable output, and undesirable output can have reduced energy input and undesirable output while fixing desirable output as shown in Figure 5. The energy and environmental production technology can be represented by the energy and environmental input set:

$$\mathbf{L}(y) = \{(e, b):\ (e, b)\ \text{ can produce } y\} \tag{29}$$

Suppose that one production unit's activities are observed with two points $a\ (e^t, y^t, b^t)$ and $a'(e^{t+1},\ y^{t+1}, b^{t+1})$ at periods "t" and "t+1" respectively. frontier^t represents the production frontier at period "t". frontier^B denotes the biennial production frontier of pooled observations from period "t" and "t+1", and frontier^B could be completely determined by frontier^{t+1} which implies that frontier^B = frontier^{t+1} . Considering $y^{t+1} \geq y^t$ with the coordinate y, production frontiers in blue lines (i.e., cross section with $y = y^{t+1}$) are higher than those in red lines (i.e., cross section with $y = y^t$) as a result of technological progress. We express the biennial Luenberger index as follows:

$$\begin{aligned} EEPI_B^{t,t+1} &= (a-d)-(a'-i) \\ effch_B^{t,t+1} &= (a-c)-(a'-i) \\ techch_B^{t,t+1} &= \{(a-d)-(a-c)\}-\{(a'-i)-(a'-i)\} \\ &= (c-d) \end{aligned} \tag{30}$$

Given $(a-c) < (a'-i)$, as shown in Fig. 5, the catch up effect becomes weak and the technical efficiency deteriorates, which indicates that relative deterioration occurs. However, considering $(a-d) > (a'-i)$, a' is closer to frontier^B than a, which implies that the EEP for observed production activity improves from period t to t+1.

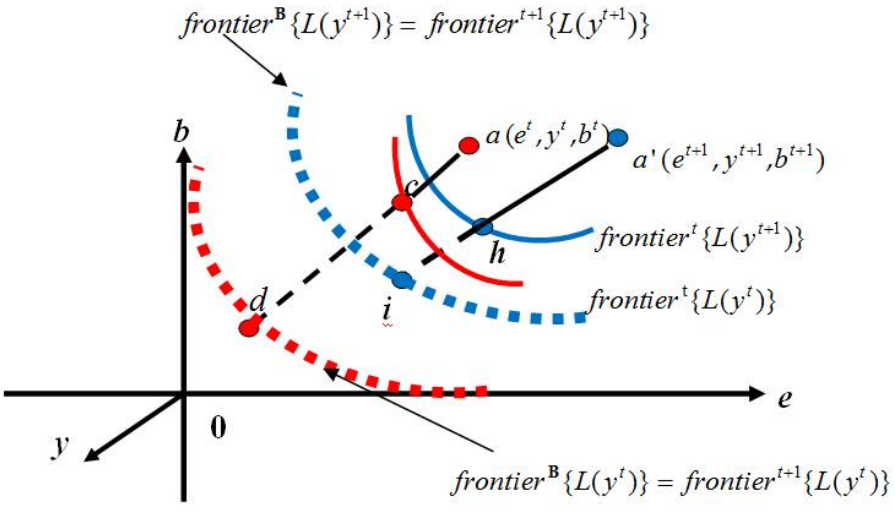

Figure 5. Deterioration of technical efficiency

Table 4 shows the contributions of specific energy and undesirable output to the changes in total performance and sub-performances. Energy plays a more important role (contribution over 50%) than undesirable outputs in total performance change and its four sub-performances. With respect to undesirable outputs, SO_2 performance change has the strongest effect on total performance change (25.36%) while the effect of soot emission performance change is the lowest (0.80%). Technological

Preprints (www.preprints.org) | NOT PEER-REVIEWED | Posted: 6 June 2018 doi:10.20944/preprints201806.0080.v1

Peer-reviewed version available at Sustainability 2018, 10, 2303; doi:10.3390/su10072303

change behaves similarly; SO_2 technological change contributes more to total technological change (26.91%) than soot technological change (4.15%). Technical efficiency change shows much different characteristics. The contribution from wastewater technical efficiency change to total technical efficiency change was the smallest (4.74%) while SO_2 technical efficiency change made the largest contribution (28.64%). In effect, SO_2 has become the largest contributor to total performance change and sub-performance changes among the three undesirable outputs.

Table 4. Contributions of specific energy and undesirable output to total performance change, sub-performance changes

Index	$EEPI_{total}^{t,t+1}$	$EEPI_{energy}^{t,t+1}$	$EEPI_{SO2}^{t,t+1}$	$EEPI_{soot}^{t,t+1}$	$EEPI_{wastewater}^{t,t+1}$
Average	0.0238	0.0123	0.0061	-0.0002	0.0055
Contribution	100%	51.01%	25.36%	0.80%	22.83%
Index	$effch_{total}^{t,t+1}$	$effch_{energy}^{t,t+1}$	$effch_{SO2}^{t,t+1}$	$effch_{soot}^{t,t+1}$	$effch_{wastewater}^{t,t+1}$
Average	-0.0157	-0.0086	-0.0045	-0.0018	-0.0007
Contribution	100%	54.97%	28.64%	11.65%	4.74%
Index	$techch_{total}^{t,t+1}$	$techch_{energy}^{t,t+1}$	$techch_{SO2}^{t,t+1}$	$techch_{soot}^{t,t+1}$	$techch_{wastewater}^{t,t+1}$
Average	0.0395	0.0210	0.0106	0.0016	0.0063
Contribution	100%	53.09%	26.91%	4.15%	15.85%

3.2.2.2. Regional Level

China can be divided into four areas by economic development levels and geographical characteristics: eastern, northeastern, central, and western areas. Urban agglomeration, considered to be an economic growth point, leads regional economic development. We explored the regional differences in urban agglomeration accordingly. The ten agglomerations we observed include Beijing-Tianjin-Hebei, the central and southern of Liaoning province, the Yangtze River Delta, the western side of the Taiwan Strait, the Shandong Peninsula, the Central Plain, the middle Yangtze River, the Pearl River Delta, Sichuan and Chongqing, and the Central Shaanxi Plain [62, 63].

Table 5 shows the average changes in EEPI and its decompositions among the four areas for every two consecutive years. The average changes in EEP are positive indicating a marked improvement in the four areas over the study period. The central area shows the most significant performance improvement (2.97%), followed by the eastern (2.73%) and western (1.96%) areas. The northeastern area experienced almost no EEP change (0.50%). Heavy industry renders the northeastern area less able to improve its EEP. We also found that the eastern area achieved the greatest technological progress (5.86%) while experiencing the greatest decline in technical efficiency (-3.14%) among the four areas; technological progress in the eastern area makes a greater contribution to performance improvement, which substantially offsets the deterioration of technical efficiency.

Table 5. Arithmetic means for $EEPI_{total}^{t,t+1}$, $effch_{total}^{t,t+1}$ and $techch_{total}^{t,t+1}$ in 2010-2014 among four areas

Arithmetic mean	$EEPI_{total}^{t,t+1}$	$effch_{total}^{t,t+1}$	$techch_{total}^{t,t+1}$
East	0.0273	-0.0314	0.0586
Central	0.0297	-0.0081	0.0378
West	0.0196	-0.0032	0.0228
Northeast	0.0050	-0.0215	0.0264

We next compared the effects of specific energy and undesirable output on the changes in total performance and sub-performances in the four areas and ten urban agglomerations. Figure 6 shows the contributions from specific energy and undesirable outputs to total performance change among four areas and ten urban agglomerations. Energy contribution rates in the eastern (50.93%), central

(51.79%), and northeastern (88.20%) areas explain more than half of the performance improvement but less so in the western area (45.38%). Most sub-performances in the four areas were improved. Soot emission performance declined in eastern and northeastern areas over 2010-2014, likely because the environmental regulation for soot emissions was eased during the study period in line with the truth that severe haze happened frequently in China. In the 10th FYP period, the central government placed quantified constraints on soot emission which were canceled in the 11th and 12th FYP periods; the top priority for the central government with mixed environmental regulations was to curb excessive emissions of SO_2 and NO_X.

Energy is apparently the major driving force for improving total performance in the Beijing-Tianjin-Hebei region, where energy accounts for 95.68% of the improvement in total performance. Energy contributed 80.64% to the improvement in total performance in the central Shaanxi plain, which is an important coal base in China. Most urban agglomerations achieved significant improvement in total performance during 2010-2014, especially the middle Yangtze River. Total performance declined i n the central and southern Liaoning province, however, due to the deterioration in soot emission performance. Total performance in the Pearl River Delta also declined due to a rapid increase in energy consumption.

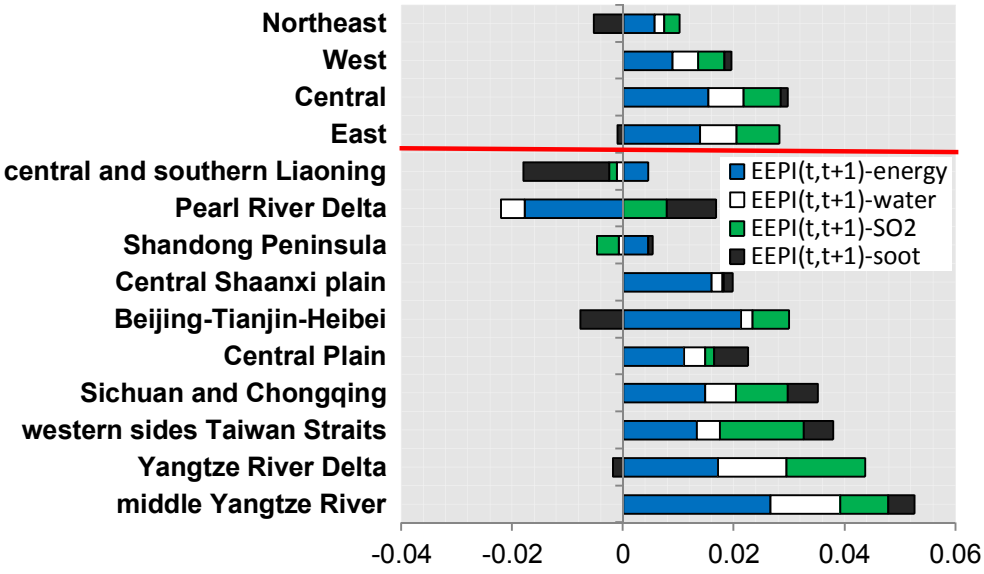

Figure 6. Contributions of specific energy and undesirable outputs performance to total performance among four areas and ten urban agglomerations

Figure 7 shows contributions from specific energy and undesirable outputs to the total technical efficiency change among the four areas and ten urban agglomerations. Total technical efficiency decreased significantly in all four regions. Deterioration in energy technical efficiency is the root cause of decline in total technical efficiency in the four areas with exception of the central area, which is defined by a decrease in SO_2 technical efficiency (elsewhere the second-most important cause of decline). Technical efficiency in most urban agglomerations decreased continually from 2010 to 2014. Only the middle Yangtze River area and central Shaanxi plain made progress in technical efficiency, which can be attributed to improvements in energy efficiency.

Preprints (www.preprints.org) | NOT PEER-REVIEWED | Posted: 6 June 2018 doi:10.20944/preprints201806.0080.v1

Peer-reviewed version available at Sustainability 2018, 10, 2303; doi:10.3390/su10072303

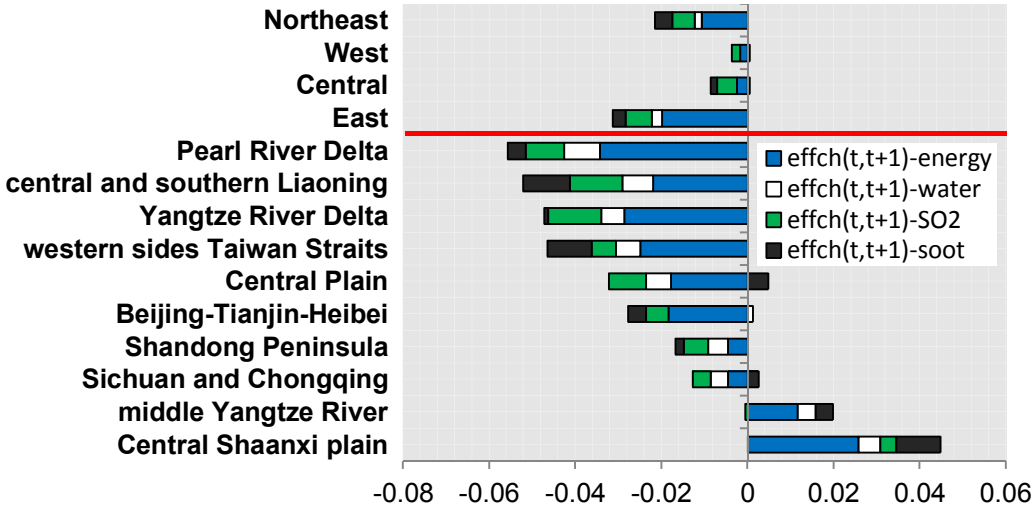

Figure 7. Contributions of specific energy and undesirable outputs to total technical efficiency among four areas and ten urban agglomerations

Figure 8 shows the contributions of specific energy and undesirable outputs to total technological change among the four areas and ten urban agglomerations. Energy contributed more significantly than the sum of undesirable outputs in the total technological change in the four areas; SO_2 technology was markedly improved while soot technology only slightly so. Technical progress in almost all ten urban agglomerations (except the central Shaanxi) grew continually. Total technological change in the central Shaanxi area declined 2.5% on average due to the bad performance of best performers around the central Shaanxi area.

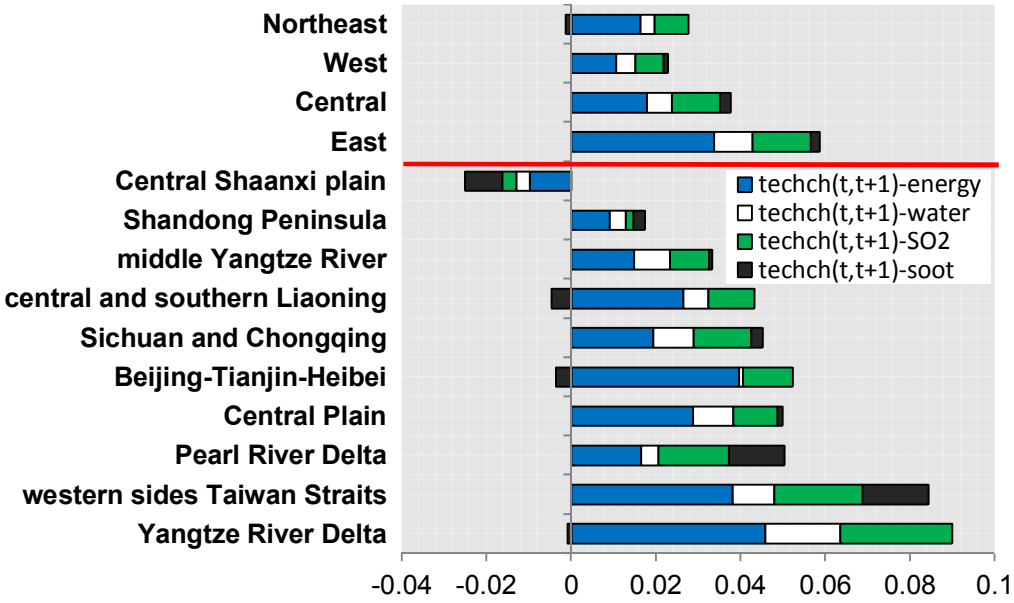

Figure 8. Contributions of specific energy and undesirable outputs to total technological change among four areas and ten urban agglomerations

3.2.3. Analysis of Spatial Distribution Evolution on Energy and Environmental Performance Potential

3.2.3.1. EEP Spatial Pattern

The average value of global Moran's I_g is 0.0807, indicating a positive spatial correlation. The positive difference in EEP spatial distribution increases along with the decline of global Moran's I_g.

Preprints (www.preprints.org) | NOT PEER-REVIEWED | Posted: 6 June 2018 doi:10.20944/preprints201806.0080.v1

Peer-reviewed version available at Sustainability 2018, 10, 2303; doi:10.3390/su10072303

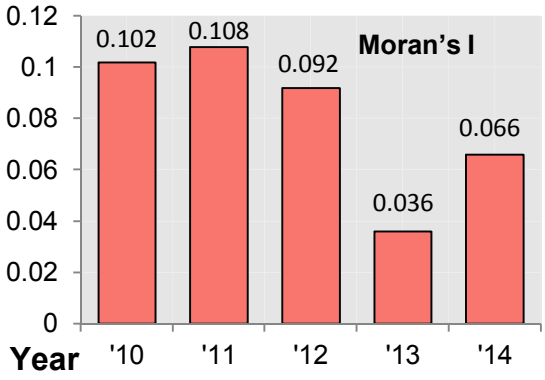

Figure 9. Changes in global Moran's I_g of EEP

We used a LISA cluster map based on the local Moran's I_l to observe the spatial agglomeration effects, i.e., whether a spatial unit shows a spatial correlation with its neighbors or not (Figure 10). There is significant agglomeration effect evidenced by four types of spatial correlations: high-high, low-low, low-high (middle is low and surroundings are high) and high-low (middle is high and surroundings are low). The high-high type mainly exists in the Huanghe Delta and the developed southeast coast of China in 2010. The high-high type areas spread from the developed southeast coast to the areas with high ecological quality, such as the northern border between Sichuan and Hubei provinces (which have a famous giant panda habitat called the Shennongjia National Nature Reserve) or the Dongting lake basin (the third-largest lake in China renowned for its beautiful scenery in the north of Hunan province); China's second largest lake, Poyang, is located in the northern Jiangxi province with a forest acreage over 60%; the Huanghe Delta and Yangtze River Delta similarly have rich wetland resources which maintain the high-high cluster characteristics resulting from their inherently high ecological quality. Cities with high ecological quality, especially those with national nature reserves, wetlands and forests, most commonly feature high-high type correlations.

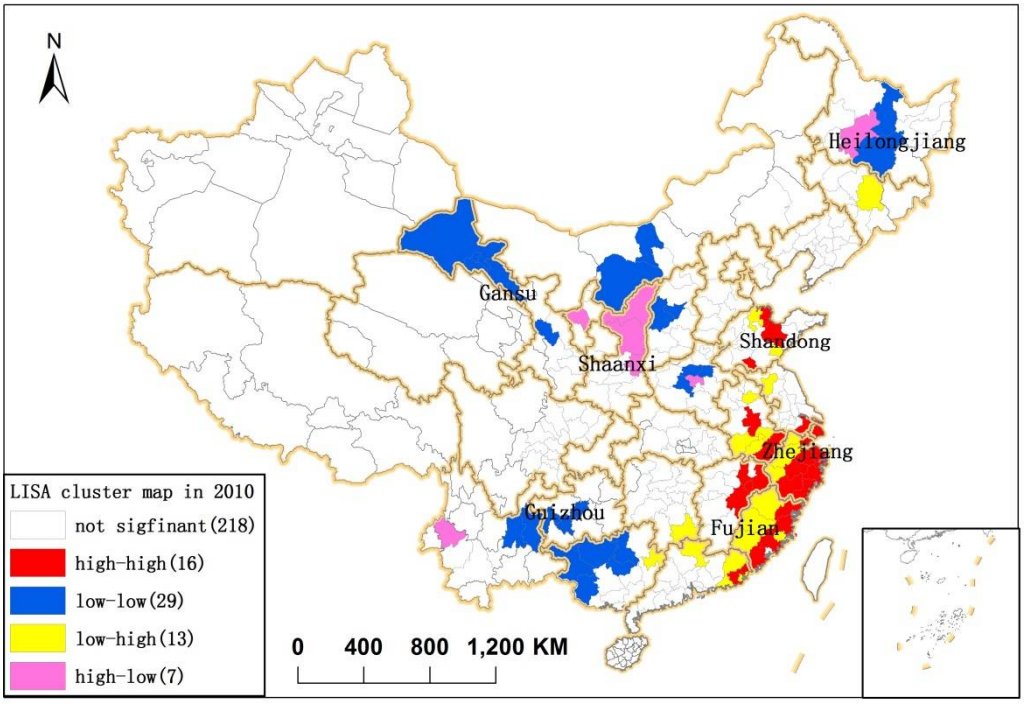

(a) LISA cluster map in 2010

Preprints (www.preprints.org) | NOT PEER-REVIEWED | Posted: 6 June 2018 doi:10.20944/preprints201806.0080.v1

Peer-reviewed version available at Sustainability 2018, 10, 2303; doi:10.3390/su10072303

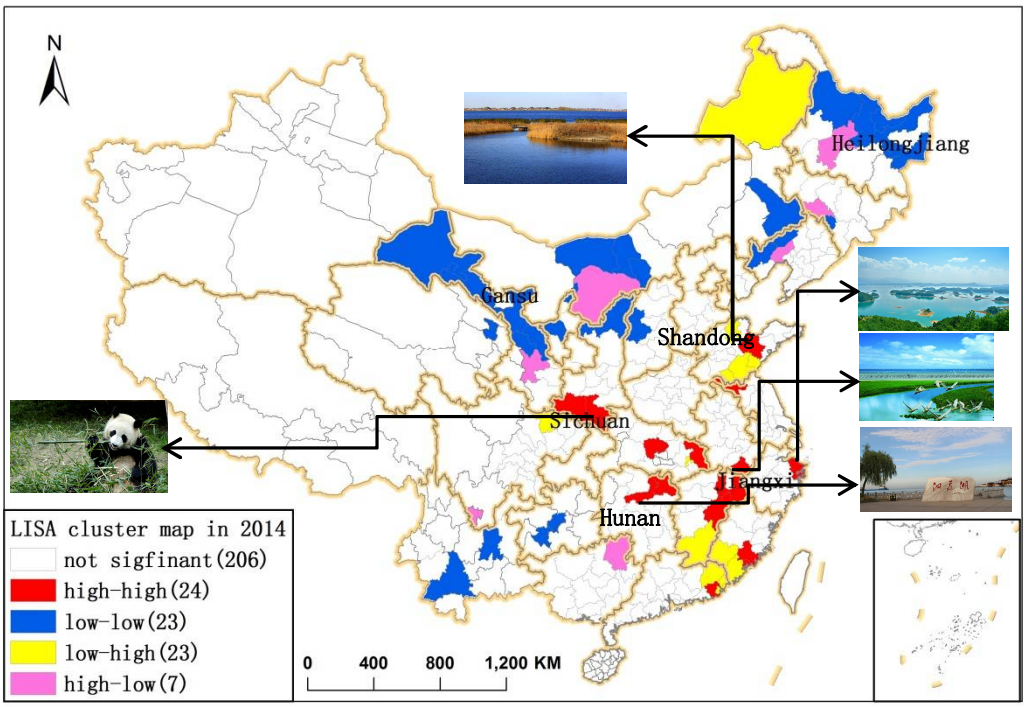

(b) LISA cluster map in 2014

Figure 10. LISA cluster map of EEP in 2010 and 2014

3.2.3.2. Influencing Factors on Energy and Environmental Performance Potential

Considering the spatial heterogeneity, we used the GWR method instead of the ordinary (global) linear regression to capture influencing factors on EEP potential with the aim to reveal its spatially varying links. Energy is positively correlated with pollutants because pollutants mainly originate in the combustion of energy sources. Energy conservation potential and SO_2 emission abatement potential exhibit similar distribution characteristics for this reason. In this study, we focused on the influencing factors of SO_2 emission abatement potential:

$$Potential_{\boldsymbol{SO_2}} = D^t_{SO_2}(\mathbf{x}^t, \mathbf{e}^t, \mathbf{y}^t, \mathbf{b}^t; \mathbf{g}) \times SO_2\ Emission \quad (31)$$

We used three key factors to interpret the change in SO_2 emission abatement potential: gross industrial output, pollution intensity, and industrial structure. Here, the ratio of SO_2 emission to gross industrial output represents pollution intensity; the industrial structure is measured by the share of GDP of the service industry [43, 64, 65]. The following GWR model was used to investigate the effects of various influencing factors on SO_2 emission abatement potential:

$$Potential_{\boldsymbol{SO_2}_i} = \beta_0(u_i, v_i) + \beta_1(u_i, v_i)GIO_i + \beta_2(u_i, v_i)SI_i + \beta_3(u_i, v_i)SR_i + \varepsilon_i \quad (32)$$

where β denotes the coefficient parameter; ε is a random error term; GIO denotes the gross industrial output; SR denotes the share of GDP of the service industry; SI represents SO_2 pollution intensity.

As shown in Table 6, Model (32) passes the 1% level significance test. The R^2 indicator of goodness of fit is 0.67 (R^2 in global regression result is 0.20), which is fairly high. The range of local R^2 is between 0.36 and 0.9.

Table 6. Overall fitting results GWR model based on SO_2 emission abatement potential

Indicator	SO_2 emission abatement potential

local R^2	0.36-0.90
R^2	0.67
adjusted R^2	0.57
residual sum of squares	5.17 E+10
AICc	6322
F	4.84
probability	0.003

Figure 11(a)-(c) shows the spatial distribution of influencing factors that affect SO_2 emission abatement potential. The natural breaks (Jenks) method was used to split the regression coefficient into four categories to ensure scientific geographical results. In most cities, the gross industrial output shows a positive effect on SO_2 emission abatement potential. Cities with larger gross industrial output need to consume more energy and are thus inclined to emit more SO_2. The strongest impact coefficients of gross industrial output are distributed in the western parts of the country. The effects of gross industrial output on SO_2 emission abatement potential also show a significant downtrend from the western interior to the eastern coast. Pollution intensity is also correlated with SO_2 emission abatement potential, because cities with higher pollution intensity produce more pollutants. Heavy industry accounts for a considerable proportion of manufacturing in areas around the Bohai Gulf. Cities in the Shandong Peninsula, central and southern Liaoning province, and Beijing-Tianjin-Hebei showed the strongest pollution intensity in terms of SO_2 emission abatement potential (i.e., areas around the Bohai Gulf where severe haze is relatively common [66-68]).

The ratio of the service industry to GDP shows an uncertain effect on SO_2 emission abatement potential. We next examined the correlation between the ratio of the service industry to GDP and SO_2 emission abatement potential with standardized z-scores, as shown in Figure 12. The Pearson correlation between them is pretty weak (0.119). Only 37 (55) cities pass the significance tests at 5% (10%) level among all 283 cities. This suggests that industrial structure is not the significant influencing factor of SO_2 emission abatement potential during our study period. In fact, improvements to industrial structure caused by relatively fast growth in the service industry do not significantly reduce SO_2 emissions. Although the ratio of manufacturing industry to GDP is decreasing on the whole, the ever-increasing value added by the manufacturing industry increases SO_2 emissions and leaves considerable room for emission abatement. This phenomenon is more common in developed cities, like Shanghai or cities in Jiangsu and Zhejiang provinces. He, et al. [69] and Hu, et al. [70] similarly found that industrial structure does not significantly affect industrial pollution at the city level in China.

Peer-reviewed version available at Sustainability 2018, 10, 2303; doi:10.3390/su10072303

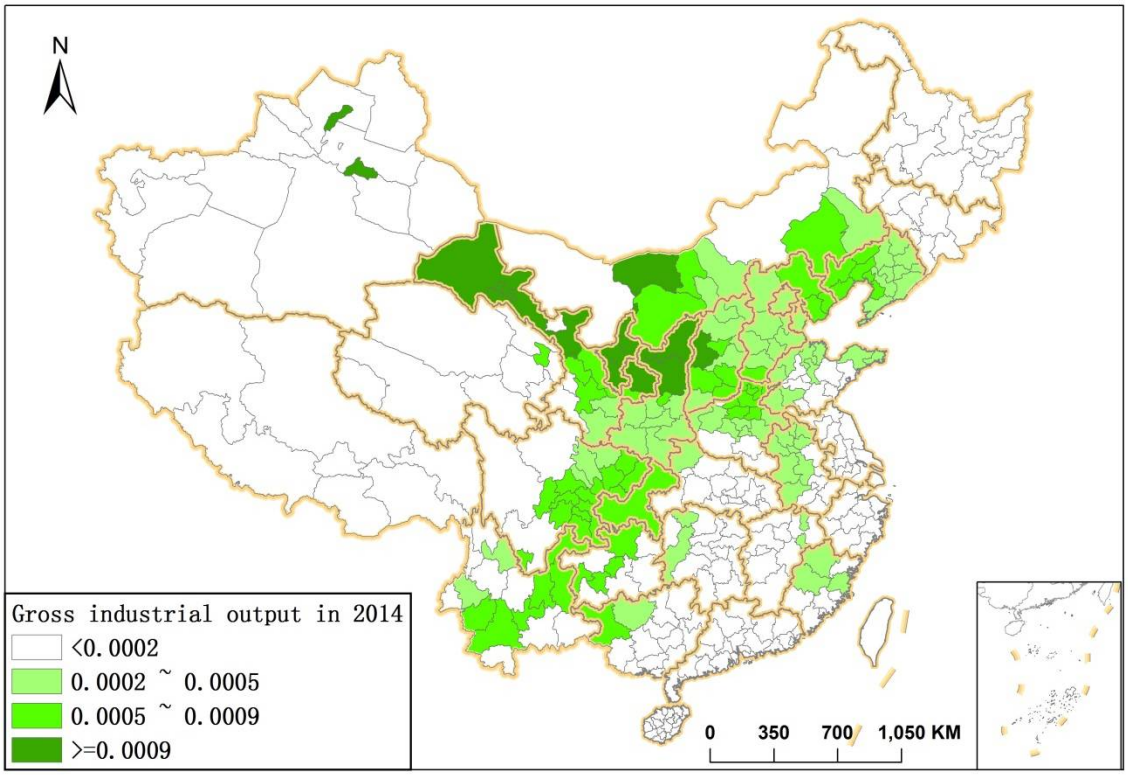

582

(a) Regression coefficient of gross industrial output

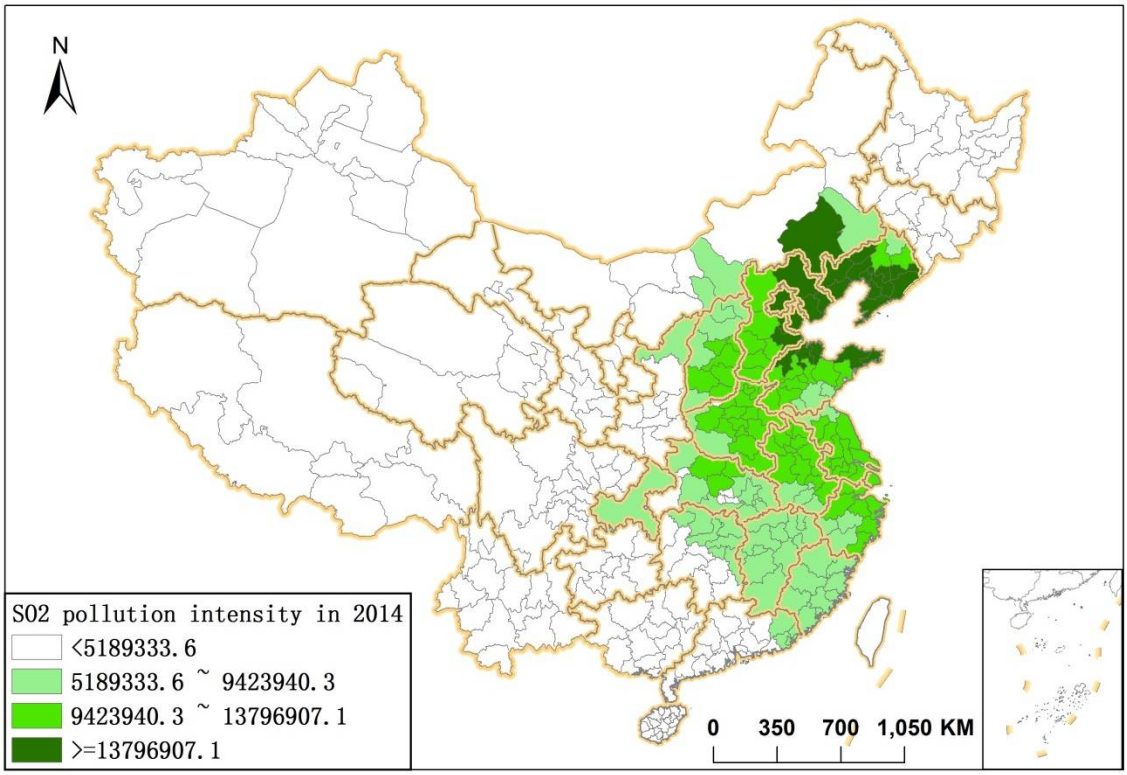

583

(b) Regression coefficient of SO_2 pollution intensity

Preprints (www.preprints.org) | NOT PEER-REVIEWED | Posted: 6 June 2018 doi:10.20944/preprints201806.0080.v1

Peer-reviewed version available at Sustainability 2018, 10, 2303; doi:10.3390/su10072303

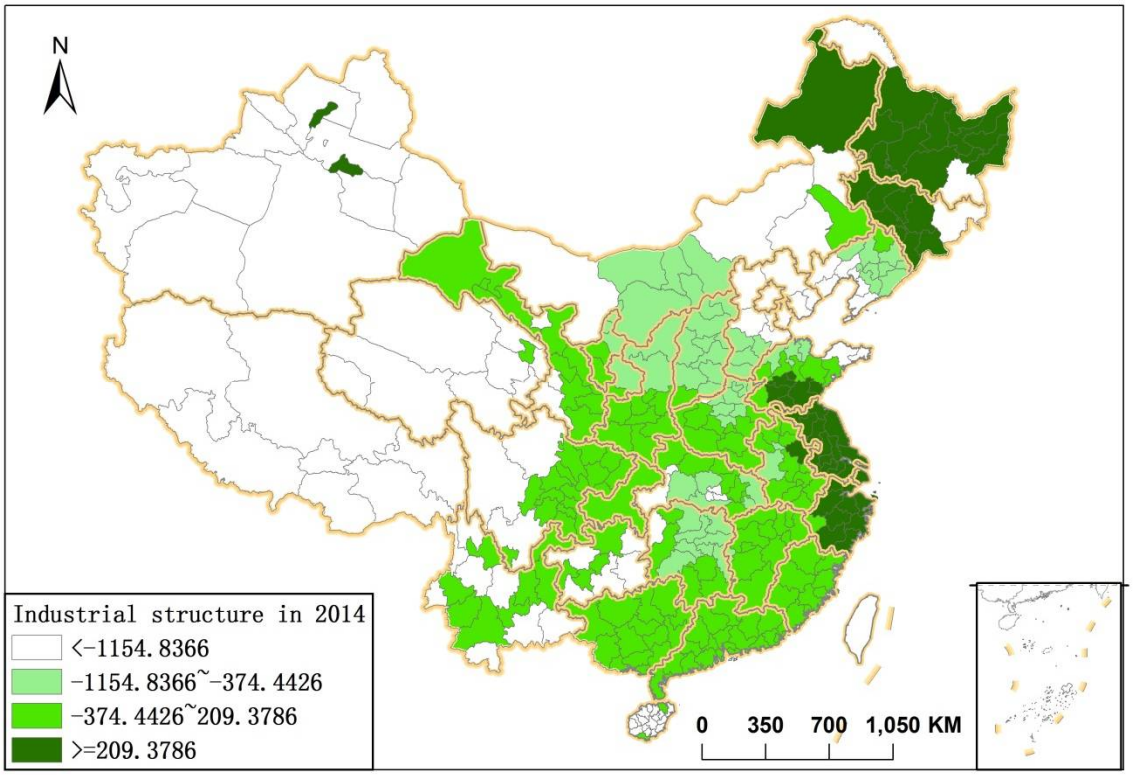

(c) Regression coefficient of industrial structure

Figure 11. Local GWR estimates of influencing factors for SO_2 emission abatement potential in 2014

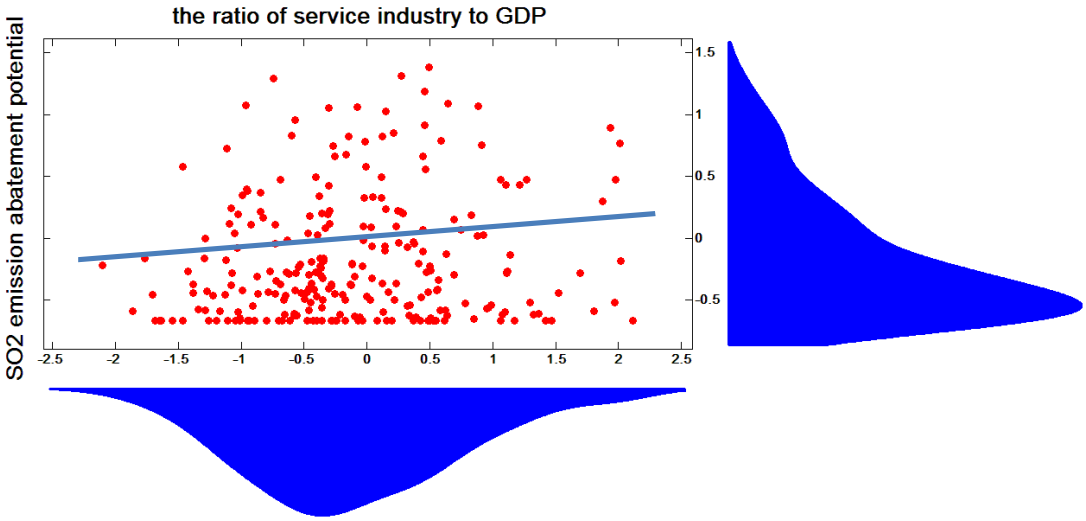

Figure 12. Correlation between ratio of service industry to GDP and SO_2 emission abatement potential

4. Conclusions

China is currently facing a trade-off between economic development and environmental protection. Chinese cities represent complete, independent administrative districts which implement environmental regulations; top administrators are held accountable for environmental damages. A given city's energy utilization and environment regulation directly influence the amount to which it pollutes the environment, and to identify the best performer and regional difference on EEP will

stimulate the cities to learn from each other. This paper proposed a new biennial Luenberger EEPI to avoid infeasibility problem in conducting data envelopment analysis. Changes in EEP were decomposed into technical efficiency change and technological change. To examine the contributions of specific undesirable outputs (e.g., SO_2, soot, and wastewater) and energy inputs to the EEP, the total performance was divided into sub-performances via a non-radial measure. We empirically analyzed a sample of 283 cities from 2010 to 2014 accordingly and investigated the primary drivers of emission abatement potential based on the GWR model. Our main conclusions can be summarized as follows.

(1) The best performers are mainly located in the Guangdong, Shandong, Jiangsu, Jiangxi, Sichuan, and Hainan provinces, while the worst performers are mainly distributed in Heilongjiang, Guangxi, Ningxia, and Shanxi provinces. The best performers possess advanced service industries and either consume less energy or have inherently high ecological quality, while the worst performers depend on abundant coal and nonferrous metal resources to support economic development. Best performers tended to move from the coastal towards the inland area over time.

(2) At the national level, average EEP change, technical efficiency change, and technological change values are 2.38%, -1.57%, and 7.90%, respectively. China achieved remarkable progress in energy conservation and emission abatement over the study period. The deterioration of the technical efficiency is a relative deterioration caused by the fast technological progress. Changes in EEP are primarily attributable to technological progress, but said progress slowed down during the study period.

(3) At the regional level, the central area (2.97%) shows the greatest improvement in total performance followed by eastern (2.73%) and western (1.96%) areas. The northeastern area (0.50%) shows almost no change in EEP. The eastern area achieves the greatest technological progress (5.86%) but greatest decline in technical efficiency (-3.14%) among the four areas. The sub-performances all increased apart from soot emission performance. Deterioration in SO_2 technical efficiency is the biggest driver of deteriorated technical efficiency in all four areas.

We used the ESDA method to find that EEP has obvious spatial agglomeration features. The high-high type clusters mainly exist in Shandong province and the southeast coast of China; high-high type clusters move from coastal areas towards the inland areas which have inherently better ecological quality. The factors that affect SO_2 emission abatement potential exhibit significant spatial heterogeneity in different areas. The gross industrial output positively affects SO_2 emission abatement potential in most cities. The strongest impact coefficients of gross industrial output are mainly distributed in the western area. Cities with the strongest positive effect of pollution intensity on SO_2 emission abatement potential were mainly distributed in central and southern Liaoning province, Beijing-Tianjin-Hebei, and Shandong Peninsula areas (i.e., areas around the Bohai Gulf which are characterized by haze problems). The ratio of service industry to GDP has an uncertain effect on SO_2 emission abatement potential, indicating that industrial structure is not the significant influencing factor of SO_2 emission abatement potential in the study period.

Acknowledgments: This work was supported by the National Natural Science Foundation of China (Grant No. 71704095).

Author Contributions: This work was designed, analyzed, and written by the both authors. The data were gathered by the corresponding author.

Conflicts of Interest: The authors declare no conflict of interest.

References

1. Song, M.; Wang, S.; Yu, H.; Yang, L.; Wu, J., To reduce energy consumption and to maintain rapid economic growth: Analysis of the condition in China based on expended IPAT model. *Renewable & Sustainable Energy Reviews* **2011,** 15, (9), 5129-5134.

643 2. British Peroleum Company. *BP Statistical Review of World Energy 2017*; British Peroleum Company：London,
644 UK,2017.
645 3. Chen, J.; Song, M.; Xu, L., Evaluation of environmental efficiency in China using data envelopment analysis.
646 *Ecological Indicators* **2015,** 52, 577-583.
647 4. Ministry of Ecology and Environmental of the People's Repuclic of China. *Report on the State of China's*
648 *Environment in 2016*; Ministry of Ecology and Environmental of the People's Repuclic of China: Beijing,
649 China, 2016.
650 5. Lepeule, J.; Schwartz, J., Chronic exposure to fine particles and mortality: an extended follow-up of the
651 Harvard Six Cities study from 1974 to 2009. *Environmental health perspectives* **2012,** 120, (7), 965-70.
652 6. Lepeule, J.; Bind, M. A.; Baccarelli, A. A.; Koutrakis, P.; Tarantini, L.; Litonjua, A.; Sparrow, D.; Vokonas,
653 P.; Schwartz, J. D., Epigenetic influences on associations between air pollutants and lung function in elderly
654 men: the normative aging study. *Environmental health perspectives* **2014,** 122, (6), 566-72.
655 7. Farrell, M. J., The Measurement of Productive Efficiency. *Journal of the Royal Statistical Society* **1957,** 120, (3),
656 253-290.
657 8. Charnes, A.; Cooper, W. W.; Rhodes, E., Measuring the efficiency of decision-making units. *European*
658 *Journal of Operational Research* **1979,** 3, (4), 339.
659 9. Kuosmanen, T.; Kortelainen, M., Measuring Eco-efficiency of Production with Data Envelopment Analysis.
660 *Journal of Industrial Ecology* **2005,** 9, (4), 59-72.
661 10. Hu, J. L.; Wang, S. C., Total-factor energy efficiency of regions in China. *Energy Policy* **2006,** 34, (17), 3206-
662 3217.
663 11. Song, M.; Yang, L.; Wu, J.; Lv, W., Energy saving in China: Analysis on the energy efficiency via bootstrap-
664 DEA approach. *Energy Policy* **2013,** 57, 1-6.
665 12. Özkara, Y.; Atak, M., Regional total-factor energy efficiency and electricity saving potential of
666 manufacturing industry in Turkey. *Energy* **2015,** 93, 495-510.
667 13. Feng, C.; Wang, M., Analysis of energy efficiency and energy savings potential in China's provincial
668 industrial sectors. *Journal of Cleaner Production* **2017,** 164.
669 14. Zhou, D. Q.; Wu, F.; Zhou, X.; Zhou, P., Output-specific energy efficiency assessment: A data envelopment
670 analysis approach. *Applied Energy* **2016,** 177, 117-126.
671 15. Honma, S.; Hu, J. L., Total-factor energy productivity growth of regions in Japan. *Energy Policy* **2009,** 37,
672 (10), 3941-3950.
673 16. Wang, Q. W.; Zhou, D. Q., An empirical study on the change of total factor energy efficiency in China.
674 *Systems Engineering* **2008,** 26, (7), 74-80.
675 17. Chang, T. P.; Hu, J. L., Total-factor energy productivity growth, technical progress, and efficiency change:
676 An empirical study of China. *Applied Energy* **2010,** 87, (10), 3262-3270.
677 18. Zhang, X. P.; Cheng, X. M.; Yuan, J. H.; Gao, X. J., Total-factor energy efficiency in developing countries.
678 *Energy Policy* **2011,** 39, (2), 644-650.
679 19. Färe, R.; Grosskopf, S.; Lovell, C. A. K.; Pasurka, C., Multilateral productivity comparisons when some
680 outputs are undesirable: A nonparametric approach. *Review of Economics & Statistics* **1989,** 71, (1), 90-98.
681 20. Kortelainen, M., Dynamic environmental performance analysis: A Malmquist index approach. *Ecological*
682 *Economics* **2008,** 64, (4), 701-715.
683 21. Zhou, P.; Ang, B. W.; Poh, K. L., Measuring environmental performance under different environmental
684 DEA technologies. *Energy Economics* **2008,** 30, (1), 1-14.

685 22. Zhang, N.; Choi, Y., Total-factor carbon emission performance of fossil fuel power plants in China: A
686 metafrontier non-radial Malmquist index analysis. *Energy Economics* **2013,** 40, (2), 549-559.
687 23. Rashidi, K.; Saen, R. F., Measuring eco-efficiency based on green indicators and potentials in energy saving
688 and undesirable output abatement. *Energy Economics* **2015,** 50, 18-26.
689 24. Sueyoshi, T.; Goto, M., Environmental assessment on coal-fired power plants in U.S. north-east region by
690 DEA non-radial measurement. *Energy Economics* **2015,** 50, (8), 125-139.
691 25. Xie, B. C.; Duan, N.; Wang, Y. S., Environmental efficiency and abatement cost of China's industrial sectors
692 based on a three-stage data envelopment analysis. *Journal of Cleaner Production* **2016,** 153.
693 26. Molinos-Senante, M.; Maziotis, A.; Sala-Garrido, R., The Luenberger productivity indicator in the water
694 industry: An empirical analysis for England and Wales. *Utilities Policy* **2014,** 30, (9), 18-28.
695 27. Managi, S., Luenberger and Malmquist productivity indices in Japan, 1955–1995. *Applied Economics Letters*
696 **2003,** 10, (9), 581-584.
697 28. Mahlberg, B.; Sahoo, B. K., Radial and non-radial decompositions of Luenberger productivity indicator
698 with an illustrative application. *International Journal of Production Economics* **2011,** 131, (2), 721-726.
699 29. Azad, M. A. S.; Ancev, T., Measuring environmental efficiency of agricultural water use: A Luenberger
700 environmental indicator. *Journal of Environmental Management* **2014,** 145, (145C), 314-320.
701 30. Wang, K., Evaluation and decomposition of energy and environmental productivity change using DEA.
702 **2016**.
703 31. Wang, K.; Wei, Y. M., Sources of energy productivity change in China during 1997–2012: A decomposition
704 analysis based on the Luenberger productivity indicator. *Energy Economics* **2016,** 54, 50-59.
705 32. Xian, Y.; Huang, Z., Sources of carbon productivity change: A decomposition and disaggregation analysis
706 based on global Luenberger productivity indicator and endogenous directional distance function. *Ecological*
707 *Indicators* **2016,** 66, 545-555.
708 33. Wang, K.; Wei, Y. M.; Zhang, X., A comparative analysis of China's regional energy and emission
709 performance: Which is the better way to deal with undesirable outputs? *Energy Policy* **2012,** 46, 574-584.
710 34. Zhou, P.; Wang, H., Energy and CO2 emission performance in electricity generation: A non-radial
711 directional distance function approach. *European Journal of Operational Research* **2012,** 221, (3), 625-635.
712 35. Zhou, P.; Poh, K. L.; Ang, B. W., A non-radial DEA approach to measuring environmental performance.
713 *European Journal of Operational Research* **2007,** 178, (1), 1-9.
714 36. Vlontzos, G.; Niavis, S.; Manos, B., A DEA approach for estimating the agricultural energy and
715 environmental efficiency of EU countries. *Renewable & Sustainable Energy Reviews* **2014,** 40, 91-96.
716 37. Meng, F.; Su, B.; Thomson, E.; Zhou, D.; Zhou, P., Measuring China's regional energy and carbon emission
717 efficiency with DEA models: A survey. *Applied Energy* **2016,** 183, 1-21.
718 38. Geng, Z. Q.; Dong, J. G.; Han, Y. M.; Zhu, Q. X., Energy and environment efficiency analysis based on an
719 improved environment DEA cross-model: Case study of complex chemical processes. *Applied Energy* **2017,**
720 205, 465-476.
721 39. Wang, J.; Zhao, T., Regional energy-environmental performance and investment strategy for China's non-
722 ferrous metals industry: a non-radial DEA based analysis. *Journal of Cleaner Production* **2016**.
723 40. Perez, K.; González-Araya, M. C.; Iriarte, A., Energy and GHG emission efficiency in the Chilean
724 manufacturing industry: Sectoral and regional analysis by DEA and Malmquist indexes. *Energy Economics*
725 **2017,** 66.
726 41. Satterthwaite, D., Cities' contribution to global warming: notes on the allocation of greenhouse gas
727 emissions. Environ Urban 20(2):539. *Environment & Urbanization* **2008,** 20, (2), 539-550.

42. Harris, P. G.; Chow, A. S. Y.; Symons, J., Greenhouse gas emissions from cities and regions: International implications revealed by Hong Kong. *Energy Policy* **2012,** 44, (44), 416-424.
43. Li, X. G.; Yang, J.; Liu, X. J., Analysis of Beijing's environmental efficiency and related factors using a DEA model that considers undesirable outputs. *Mathematical & Computer Modelling* **2013,** 58, (5-6), 956-960.
44. Yuan, P.; Cheng, S.; Sun, J.; Liang, W., Measuring the environmental efficiency of the Chinese industrial sector: A directional distance function approach. *Mathematical & Computer Modelling* **2013,** 58, (5-6), 936-947.
45. Wang, Q.; Zhao, Z.; Shen, N.; Liu, T., Have Chinese cities achieved the win–win between environmental protection and economic development? From the perspective of environmental efficiency. *Ecological Indicators* **2015,** 51, 151-158.
46. Zhou, D. Q.; Wang, Q.; Su, B.; Zhou, P.; Yao, L. X., Industrial energy conservation and emission reduction performance in China: A city-level nonparametric analysis. *Applied Energy* **2016,** 166, 201-209.
47. Guo, J.; Zhu, D.; Wu, X.; Yan, Y., Study on Environment Performance Evaluation and Regional Differences of Strictly-Environmental-Monitored Cities in China. *Sustainability* **2017,** 9, (12), 2094.
48. Färe, R.; Grosskopf, S., Directional distance functions and slacks-based measures of efficiency. *European Journal of Operational Research* **2010,** 200, (1), 320-322.
49. Pastor, J. T.; Asmild, M.; Lovell, C. A. K., The biennial Malmquist productivity change index. *Socio-Economic Planning Sciences* **2011,** 45, (1), 10-15.
50. Chambers, R. G.; Chung, Y.; Färe, R., Benefit and distance functions. *Journal of Economic Theory* **1995,** 70, (2), 407-419.
51. Wang, H.; Zhou, P.; Zhou, D. Q., Scenario-based energy efficiency and productivity in China: A non-radial directional distance function analysis. *Energy Economics* **2013,** 40, (2), 795-803.
52. Getis, A.; Ord, J. K., *The analysis of spatial association by use of distance statistics*. *Springer Berlin Heidelberg*: 2010; p 127-145.
53. Brunsdon, C.; Fotheringham, A. S.; Charlton, M. E., Geographically weighted regression: A method for exploring spatial nonstationarity. *Geographical Analysis* **1996,** 28, (4), 281-298.
54. Fotheringham, A. S.; Brunsdon, C.; Charlton, M., *Geographically weighted regression: The analysis of spatially varying relationships*. *International Union of Crystallography*: 2002; p C125-C126.
55. Brunsdon, C.; Fotheringham, A. S.; Charlton, M., Geographically weighted summary statistics— a framework for localised exploratory data analysis. *Computers Environment & Urban Systems* **2002,** 26, (6), 501-524.
56. National Bureau of Statistics of the People's Republic of China. *The China City Statistical Yearbook 2011-2015*; National Bureau of Statistics of the People's Republic of China: Beijing, China，2011-2015.
57. National Bureau of Statistics of the People's Republic of China. *The China Provincial Statistical Yearbook 2011-2015*; National Bureau of Statistics of the People's Republic of China: Beijing, China, 2011–2015.
58. Quah, D., Empirical cross-section dynamics in economic growth. *Discussion Paper* **1992,** 37, 426-434.
59. Quah, D., Empirics for economic growth and convergence. *Cepr Discussion Papers* **1996,** 40, (6), 1353–1375.
60. Quah, D. T., Empirics for growth and distribution: stratification, polarization, and convergence clubs. *Journal of Economic Growth* **1997,** 2, (1), 27-59.
61. Meng, F. Y.; Fan, L. W.; Zhou, P.; Zhou, D. Q., Measuring environmental performance in China's industrial sectors with non-radial DEA. *Mathematical & Computer Modelling* **2013,** 58, (5-6), 1047-1056.
62. Deng, L. J.; Zhang, P. Y.; Ping, L. I., Equilibrium of population and economic development in the top ten urban agglomerations in China. *Journal of the Graduate School of the Chinese Academy of Sciences* **2010**.

770 63. Zeng, P.; Chen, F., Empirical research of "energy-environment-economy" comprehensive accounting
771 system of the top ten urban agglomerations in china. *Forum on Science & Technology in China* **2012**.
772 64. Peng, L.; Zhang, Y.; Wang, Y.; Zeng, X.; Peng, N.; Yu, A., Energy efficiency and influencing factor analysis
773 in the overall Chinese textile industry. *Energy* **2015,** 93, (2), 1222-1229.
774 65. Fan, Y.; Bai, B.; Qi, Q.; Peng, K.; Yue, Z.; Jing, G., Study on eco-efficiency of industrial parks in China based
775 on data envelopment analysis. *Journal of Environmental Management* **2017,** 192, 107-115.
776 66. Su, B.; Zhan, M.; Zhai, J.; Wang, Y.; Fischer, T., Spatio-temporal variation of haze days and atmospheric
777 circulation pattern in China (1961–2013). *Quaternary International* **2015,** 380-381, (15), 14-21.
778 67. Zhang, J.; Chen, J.; Xia, X.; Che, H.; Fan, X.; Xie, Y.; Han, Z.; Chen, H.; Lu, D., Heavy aerosol loading over
779 the Bohai Bay as revealed by ground and satellite remote sensing. *Atmospheric Environment* **2015,** 124.
780 68. Zhou, M.; Zhang, Y.; Han, Y.; Wu, J.; Du, X.; Xu, H.; Feng, Y.; Han, S., Spatial and temporal characteristics
781 of PM2.5 acidity during autumn in marine and coastal area of Bohai Sea, China, based on two-site contrast.
782 *Atmospheric Research* **2018,** 202.
783 69. He, C.; Huang, Z.; Ye, X., Spatial heterogeneity of economic development and industrial pollution in urban
784 China. *Stochastic Environmental Research & Risk Assessment* **2014,** 28, (4), 767-781.
785 70. Hu, Z.; Miao, J.; Miao, C., Agglomeration characteristics of industrial pollution and their influencing factors
786 on the scale of cities in China. *Dili Yanjiu（Geographical Research）* **2016,** 35, (8), 1470-1482.(in Chinese).
787
788